UNIVERISTY OF PISA

Department of Reproductive Medicine and Child Development

Ph.D THESIS

IN

Physiopathology of Reproduction and Sexology

EXTRA-NUCLEAR SIGNALING OF ESTROGEN RECEPTOR TO BREAST CANCER CYTOSKELETAL REMODELING, MIGRATION AND INVASION

Defender:

Dr. Maria Silvia Giretti

Tutor:

Dr. Tommaso Simoncini

Doctorate 2008

UNIVERISTY OF PISA

Department of Reproductive Medicine and Child Development

Ph.D THESIS

IN

Physiopathology of Reproduction and Sexology

EXTRA-NUCLEAR SIGNALING OF ESTROGEN RECEPTOR TO BREAST CANCER CYTOSKELETAL REMODELING, MIGRATION AND INVASION

Defender:

Dr. Maria Silvia Giretti

Tutor:

Dr. Tommaso Simoncini

Doctorate 2008

CONTENTS

ACKNOLEDGEMENTS...

Al mio carismatico Direttore e guida (anche sulle piste nere!...) Prof. Andrea Riccardo Genazzani.

Al mio“ illuminato” ed “ illuminante” tutor Tommaso Simoncini.

Ai “più che colleghi” membri del laboratorio MCGEL che con i loro preziosi consigli e pratici aiuti hanno permesso la realizzazione di questo progetto di ricerca.

Ai miei cari.

Al mio Fili.

SUMMARY

Background: Estrogens are established enhancers of breast cancer development and progression, but less is known on the effects on migration and metastasis. We studied the actions of estrogens on actin cytoskeleton and cell movement and invasion in breast cancer cells. Moreover, we characterized the signaling steps through which these actions are enacted

Methodology/Principal Findings: In estrogen receptor (ER) positive T47-D breast cancer cells 17β-estradiol induces rapid and dynamic actin cytoskeleton remodeling with a loss of stress fibers and the formation of the specialized membrane structures like membrane ruffles, pseudopodia and lamellipodia. These effects depend on the rapid activation of the actin-binding protein moesin. Moesin activation by estradiol is related to the interaction of ERα with the G protein $G\alpha_{13}$, which results in the recruitment of the small GTPase RhoA and in the subsequent activation of its downstream effector Rho-associated kinase-2 (ROCK-2). ROCK-2 is responsible for moesin phosphorylation. The recruitment of the $G\alpha_{13}$/RhoA/ROCK/moesin cascade is necessary for the enhancement of breast cancer cell horizontal migration and invasion of three-dimensional matrices by estrogen. In addition, human samples of normal breast tissue, benign fibroadenomas and invasive ductal carcinomas show that the expression of wild-type moesin as well as of its active form is deranged in cancers, with increased protein amounts and a loss of association with the cell membrane.

Conclusions/Significance: These results provide an original mechanism through which estrogen can alter the progression of breast cancer, identifying the nongenomic $G\alpha_{13}$/RhoA/ROCK/moesin signaling cascade as a target of ERα in breast cancer cells. This information helps to understand the effects of estrogens on breast cancer metastasis and they may provide new targets for therapeutic interventions.

INTRODUCTION

One out of eight women develop breast cancer at some stage throughout life (1). Despite the recent improvements in survival rates, many patients relapse, and the majority of these patients die for disseminated metastatic disease, which supports the need for new therapeutic strategies.

In the mammary gland, the sex steroid estrogen promotes breast growth and development at puberty and during the menstrual cycle and pregnancy (2). In addition to these physiological effects, estrogen plays a major role in the development and progression of breast cancer. Prolonged exposure to estrogen, i.e. early menarche, late menopause or postmenopausal hormone replacement therapy, is associated with a greater risk of developing breast cancer (3). Estrogen promotes breast cancer proliferation through a number of well established pathways (4). On the contrary, the effects of estradiol on tumor cell motility and invasion are poorly understood.

Cell movement is a highly integrated molecular process that plays a central role in a wide variety of biological phenomena, representing a key aspect of many normal and abnormal processes (5). In embryogenesis, cell migration is a recurring phenomenon in important morphogenic events ranging from gastrulation to the development of the nervous system (6). Cell motility is also prominent in the adult organism, in physiological and pathological conditions. For example, cell movement is required in the inflammatory and immune response for leukocytes or lymphocytes to migrate into tissues (7). Wound healing requires fibroblast and vascular endothelial cell movement to achieve tissue repair. Angiogenesis requires movement of vascular cells, as well. Even more importantly, cell movement is the basis for local cancer invasion and distant metastasis, which represent the main reason of morbidity and mortality for malignancies (8).

Although the cellular mechanisms behind cell movement are extremely complex, a critical role in the generation of motility force is played by the dynamic remodelling of the actin cytoskeleton, which forms the backbone of every cell (9). In addition to this, dynamic changes of the cytoskeleton are related to the ability of the cell to respond to external signals from the surrounding environment and result in the recruitment of specific intracellular signalling cascades.

The cytoskeleton is an organized structure formed by the connection of three different types of filaments: actin, microtubules and intermediate filaments. These cytoskeletal complexes interact together as a dynamic network contributing to cell functions such as structural integrity, shape,

division and cell motility. Indeed, in most animal cells, the cytoskeleton is the primary actor in creating the driving forces through which cells move(10) (11). Actually, although other non-actin cytoskeletal complexes aid in coordinating cell movement and in empowering translocation, the actin cytoskeleton through highly dynamic remodelling and continuous creation of new actin networks is considered essential for pushing the cell forward in the surrounding environment(12), especially at front-membrane cell protrusions that allow the very first steps of cell motility. This restructuring of cell shape is achieved with the help of a number of accessory proteins and signaling pathways (12) that mediate signals of growth factor and cytokines.

In this context, we have recently described how the rapid exposure of human endothelial cells to physiological level of estradiol leads to a rapid remodelling of actin cytoskeleton with a loss of stress fibres and the formation of cortical actin complexes (13).This cytoskeletal rearrangement, associated with the development of specialized cell membrane structures such as ruffles and pseudopodia, is obtained through the activation of the actin-regulatory protein, moesin (13). A number of studies have underlined the fundamental contribution of the ezrin-radixin-moesin (ERM) family of proteins to cytoskeletal processes responsible for many vital cellular functions such as cell motility(14).We have described how the activation of moesin is rapidly triggered by a complex of non-genomic intracellular events that requires the interaction of ERα with the G protein Gα13 with the following involvement of the ubiquitous cytoskeletal modulator RhoA and of the Rho-associated kinase, ROCK, which is responsible for the phosphorylation of moesin (13).

Moesin belongs to the ezrin-radixin-moesin (ERM) family of actin-binding proteins (15). By interacting with actin, activated ERMs induce actin de-polymerization and re-assembly toward the cell membrane edge, supporting the formation of cortical actin complexes (16). These complexes help the formation of molecular bridges between the actin cytoskeleton, integrins and focal adhesion complexes within ruffles and pseudopodia and are critical for cell movement (12).

Ezrin, another member of the ezrin/radixin/moesin (ERM) family, is over-expressed in highly aggressive sarcomas (14, 17), as well as in breast cancer, being associated with higher metastasis rate (18). In addition, ezrin expression is induced by estrogens in ovarian cancer cells (19) suggesting that ERM proteins might have important functions in cancer progression and/or metastasis.

In addition, a large amount of literature supports a key role of the Rho family of GTPases (Rho, Rac and CDC42) in co-ordinately regulating the polymerization of the actin cytoskeleton and of focal

adhesion turnover during cell migration (20) through the activation of different downstream effectors such as PI3K (phosphoinositide-3 kinase), PTEN phosphatase (wich converts phosphoinositides PIP_3 into PIP_2) and the WASP (Wiskott-Aldrich syndrome protein) family of proteins. The discovery of this group of cytoskeletal-regulatory proteins has contributed to clarify the molecular basis of cell movement. Indeed, signaling from Rho small GTPases to the Arp2/3 complex, the WASP family members WASP, N-WASP and WAVE promote the formation and branching of actin filaments (21). Furthermore, estrogen might play a pivotal role in the process of tumour invasion through the induction of a FAK-dependent intracellular cascade (22).

Estrogen administration to breast cancer cells leads to estrogen receptor-α (ERα) membrane translocation and to the rapid formation of such specialized cell membrane structures (23). Similar effects are found in human endothelial cells, where estrogen alters the cytoskeleton and increases cell migration through the activation of the actin binding protein, moesin (13). In this paper we study the effects of estradiol on the migration and invasion of ER+ or ER- breast cancer cells and we relate these observations to actin remodeling and to the activation of moesin and we characterize the signaling steps involved in these actions. In addition, we study the expression and sub-cellular localization of wild type and activated moesin in normal breast tissue, benign breast disorders as well as in ER+ and ER- invasive breast carcinomas, highlighting the relationship with lymph node metastasis.

MATERIALS AND METHODS

Cell cultures and treatments

The human breast carcinoma cell line T47-D and MDA-MB-468 were obtained from the American Type Culture Collection. T47-D cells were grown in RPMI 1640 supplemented with L-glutamine (2mM), 10% fetal bovine serum. MDA-MB-468 cells were cultured in McCoy's 5A medium with L-glutamine (2mM) and 10% fetal bovine serum. Before treatments, both breast cancer cells lines were kept 24 hours in medium containing steroid-deprived FBS. Before experiments investigating non-transcriptional effects, cancer cells were kept in medium containing no FBS for 8 hours. Whenever an inhibitor was used, the compound was added 30 minutes before starting the treatments. 17β-estradiol, 17β-estradiol-BSA, tamoxifen, PTX, Y-27632, PD98059, L-NAME and wortmannin were from Sigma-Aldrich (Saint-Louis, MO), ICI 182,780, PPT and DPN were obtained by Tocris Cookson (Avonmouth, UK).

Immunoblottings

Cell lysates were separated by SDS-PAGE. Antibodies used were: moesin (clone 38, Transduction Laboratories, Lexington, KY), Thr^{558}-P-moesin (sc-12895, Santa Cruz Biotechnology, Santa Cruz, CA), ERα (TE111, NeoMarkers, Union City, CA), ERβ (N-19, Santa Cruz), ROCK-2 (C-20, Santa Cruz), $G\alpha_{13}$ (A-20, Santa Cruz), RhoA (26C4, Santa Cruz). Primary and secondary Abs were incubated with standard technique. Immunodetection was accomplished with enhanced chemiluminescence.

Cell immunofluorescence

T47-D cells were grown on coverslips and exposed to treatments. Cells were fixed and permeabilized with methanol at -20°C for 10 min. Blocking was performed with 3% normal serum for 20 min. Cells were incubated with antibodies against human moesin (clone 38, Transduction Laboratories) or with Texas Red-phalloidin (Sigma). The nuclei were counterstained with or 4'-6-diamidino-2-phenylindole (DAPI) (Sigma) and mounted with Vectashield mounting medium (Vector Laboratories, Burlingame, CA). Immunofluorescence was visualized using an Olympus BX41 microscope and recorded with a high-resolution DP70 Olympus digital camera. After conversion to greyscale images, the cell membrane thickness and the gray levels of the extracellular area, cell membrane as well as cytoplasm were quantified using the Leica QWin image analysis and image processing software (Leica Microsystems, Wetzlar, Germany).

Co-immunoprecipitation assays

HUVEC were harvested in 100 mM Tris-HCl, pH 6.8, 4% SDS, 20% glycerol, 1 mM Na_3VO_4, 1 mM NaF, and 1 mM PMSF. Equal amounts of cell lysates were incubated with 1 μg of precipitating Ab (ERα, ROCK-2 or $G\alpha_{13}$) for 1 hour at 4°C under gentle agitation. 25 μL of a 1:1 protein A-agarose slurry were added, and the samples were rolled at 4°C for another hour. The samples were then pelleted, washed, and resuspended in 50 μL of 2X Laemmli buffer for immunoblotting.

Kinase assays

T47-D cells were harvested in 20 mM Tris-HCl, 10 mM EDTA, 100 mM NaCl, 0.5% IGEPAL, 0.1 mg/mL PMSF. Equal amounts of cell lysates were immunoprecipitated with an Ab vs. ERα or ROCK-2. The IPs were washed three times with 20 mM Tris-HCl,10 mM EDTA, 150 mM NaCl 0.1% IGEPAL, 0.1 mg/mL PMSF. Two additional washes were performed in kinase assay buffer (20 mM MOPS, 25 mM β-glycerophosphate, 5 mM EGTA, 1 mM DTT) and the samples were therefore resuspended in this buffer. 5 μg of de-phosphorylated myelin basic protein (Upstate, Lake Placid, NY) together with 500 μM ATP and 75 mM $MgCl_2$ were added to each sample and the reaction was started putting the samples at 30°C for 20 min. The reaction was stopped on ice and by resuspending the samples in Laemmli Buffer. The samples were separated with SDS-PAGE and western analysis was performed using an Ab recognizing Thr^{98}-P-myelin Basic Protein.

Rho Activity Assay

T47-D cells were treated and harvested in Mg^{2+} Lysis/Wash Buffer (125 mM HEPES, pH 7.5, 750 mM NaCl, 5% Igepal CA-630, 50 mM $MgCl_2$, 5 mM EDTA and 10% glycerol). 1 μg of proteins were used to pull-down active, GTP-bound, RhoA using Rhotekin-GSH-agarose. The IPs were washed with Mg^{2+} Lysis/Wash Buffer and therefore resuspended in 2X Laemmli buffer. The IPs were separated on a denaturing acrylamide gel and western analysis with an anti-RhoA Ab was performed.

Transient transfections

T47-D cells were transfected with each plasmid (15 μg) using the Lipofectin reagent (Invitrogen, Carlsbad, CA) according to the manufacturer's instructions. The transfected plasmids were: $G\alpha_{13}$ Q226L, $G\alpha_{13}$ Q226L/D294N, RhoA T19 and RhoA G14V, Ras G12V and Ras S17N. All the inserts were cloned in pcDNA3.1+. The constructs were obtained from the Guthrie cDNA Resource Center (www.cdna.org). As control, parallel cells were transfected with empty pcDNA3.1+ plasmid. Cells

(60-70% confluent) were treated 24 h after transfection and cellular extracts were prepared according to the experiments to be performed.

Gene silencing with RNA interference

Two synthetic small interfering RNA targeting estrogen receptor α (siRNA SMARTpool ESR1, Dharmacon, USA) were used at the final concentration of 100 nM to silence ERα according to the manufacturer's instructions. T47-D breast cancer cells were treated 60 hours after siRNA transfection. The efficacy of gene silencing was checked with western analysis and found to be optimal at 60 hours.

Moesin silencing with antisense oligonucleotides

Validated antisense phosphorotioate oligonucleotides (S-modified) (PONs) complementary to the 1-15 position of the human moesin gene coding region [31] were obtained. The sequence was 5'-TACGGGTTTTGCTAG-3' for moesin antisense PON. The complementary sense PON was used as control (5'-CTAGCAAAACCCGTA-3'). PONs transfections were performed on sub-confluent T47-D breast cancer cells. PONs were resuspended in serum-free medium with 2% Lipofectin (Invitrogen) and added to the culture medium every 12 hours at the final concentration of 4 μM. Every 24 hours T47-D cells were washed and fresh medium supplemented with 4 μM of PONs was added. Moesin silencing was assessed through protein analysis up to 72 hours following transfection.

Cell migration assay

Cell migration was assayed with razor scrape assays. Briefly, a razor blade was pressed through the confluent T47-D breast cancer cell monolayer into the plastic plate to mark the starting line. T47-D cells were swept away on one side of that line. Cells were washed, and 2.0 mL of DMEM containing steroid-deprived FBS and gelatin (1 mg/mL) were added. Cytosine β-D-arabinofuranoside hydrochloride (Sigma) (10 μM), a selective inhibitor of DNA synthesis which doesn't inhibit RNA synthesis was used 1 h before the test substance was added. Migration was monitored for 48 hours. Every 12 h fresh medium and treatment were replaced. Cells were digitally imaged and migration distance was measured by using phase-contrast microscopy.

Cell invasion assay

Cell invasion were assayed using the BD BioCoat^{TM} Growth Factor Reduced (GFR) Matrigel^{TM} Invasion Chamber (BD Bioscience, USA). In brief, after rehydrating the GFR Matrigel inserts, the

test substance was added to the wells. An equal number of Control Inserts (no GFR Matrigel coating) were prepared as control. 0.5 mL of T47-D cell suspension (2.5 x 10^4 cells/mL) were added to the inside of the inserts. The chambers were incubated for 24 h at 37°C, 5% CO_2 atmosphere. After incubation, the non-invading cells were removed from the upper surface of the membrane using cotton tipped swabs. Then the cells on the lower surface of the membrane were stained with Diff-Quick stain. The invading cells were observed and photographed under the microscope at 100 X magnification. Cells were counted in the central field of triplicate membranes. The invasion index was calculated as the % invasion test cell/% invasion control cell.

Tissue specimens

Wild-type and phosphorylated-moesin expression was investigated in 20 ductal invasive breast adenocarcinomas, stage pT1c. Five of these were ER^+/N^+, 5 were ER^+/N^-, 5 were ER^+/N^+ and 5 were ER^-/N^-. In addition, we also evaluated moesin and P-moesin in benign breast fibroadenomas (n=5) as well as in normal breast tissue (n=5). Samples were collected according to conventional histopathological diagnostic protocols and were fixed in 10% buffered formalin, embedded in paraffin, and stained with hematoxylin-eosin. Histological diagnosis and grading were performed according the *World Health Organization Classification of Tumors* (2002), and staging was determined according to the TNM system.

Immunohistochemistry

Histological sections of 4 μm were mounted on silanized slides and allowed to dry for 1 h at room temperature (RT), followed by 1 h incubation in an oven at 60°C. Briefly, after deparaffination and rehydration, epitope retrieval was performed by immersing slides in DAKO Epitope Retrival Solution (0.01 M citrate buffer, pH 6.0) in a water bath at 98°C for 40 minutes followed by a 20 minutes cool-down period at RT. The working dilution for the anti-human moesin monoclonal antibody (clone 38; BD Biosciences) was 1:50. P-moesin was evaluated with anti-P-moesin goat polyclonal antibody (Santa Cruz) at 1:50 dilution. The sections were incubated with primary antibodies for 1 hour at RT. The DAKO EnVision detection system kit was employed to detect moesin, instead for P-moesin the DAKO LSAB+ was used. Moesin and P-moesin expression were scored as positive when there was cytoplasmic, membrane or both cytoplasmic and membrane immunostaining. Staining scores were established semi-quantitatively from the percentage of $Moesin^+$ and P-$moesin^+$ cells and the staining intensity. Tumors were graded as negative (<1% positive cells), focal (low intensity, with $\geq$1% to < 30% positive cells), intense (moderate or high

intensity with diffused positive cells). Staining patterns were independently adjudicated by two pathologists.

G-actin /F-actin assay

The G-actin/F-actin assay kit was purchased from Cytoskeleton Inc (# BK037, Denver, USA). This kit is used to determine accurately the amount of filamentous actin (F-actin) content versus free globular-actin (G-actin) content in a cell population. In brief, confluent T47-D cells were harvested with lysis at 37°C and F-actin stabilization buffer (50 mM PIPES, 50 mM KCl, 5 mM $MgCl_2$, 5 mM EGTA, 5% glycerol, 0.1% Nonidet P40, 0.1% Triton X-100, 0.1% Tween 20, 0.1% 2-mercapto-ethanol, 0.001% antifoam C, 1 mM ATP) after treatments. Total protein concentration was determined by standard method. Positive and negative controls were set by adding F-actin enhancing solution (phalloidin, 1 μM) or F-actin depolymerization solution (10 μM cytochalasin-D) to the lysates, respectively. The lysates were incubated at 37°C for 10 min, followed by a centrifuge at 2000 rpm for 5 min to pellet and discard unbroken cells. Supernatant were centrifuged at 10,000 × *g* for 1 h at 37°C. After that, supernatant and pellet were both collected. Pellets were resuspended to the same volume as the supernatant using ice cold distilled water plus F-actin depolymerization solution (10 μM cytochalasin-D) and put on ice for 1 h to dissociate F-actin. According to the protein concentration previously measured, equivalent volumes of supernatant and dissolved pellet were loaded to run Western blot and G-actin/F-actin ratio was quantified using a quantitative digital imaging system.

Statistical analysis

All values are expressed as mean ± SD. Statistical differences between mean values were determined by ANOVA, followed by the Fisher's protected least significance difference (PLSD). The χ^2 test, Fisher's exact test were used to evaluate the significance of the expression pattern of moesin and p-moesin and the clinical and pathological parameters with version 12 of the SPSS software package (SPSS Inc, IL, USA). A value of $P < 0.05$ was considered significant.

RESULTS

Estrogen receptor activation induces a rapid cytoskeletal rearrangement and the development of specialized membrane structures

To assess the potential effect of estrogen receptor (ER) recruitment on breast cancer cell movement, we studied the morphological changes of the actin cytoskeleton in ER+ T47-D cells exposed to estradiol. Unstimulated cells displayed mainly longitudinally-arranged actin fibres in the cytoplasm (Fig. 1A). Recruitment of ER with 17β-estradiol (E2, 10 nM) resulted in a rapid change in actin organization, with a remodeling of the fibres toward the cell membrane edge (Fig. 1A). Plus, exposure to E2 was associated with the formation of specialized membrane structures linked to cell attachment to the extracellular matrix and to cell movement, such as pseudopodia and membrane ruffles (Fig. 1A). This phenomenon was time-dependent and transient, being maximal after 15-20 minutes and then progressively reversing to the basal arrangement between 30 and 60 minutes (Fig. 1A). The remodeling of actin fibres and the morphological changes of the membrane were quantified by assessing the intensity of the actin fluorescence after conversion of the coloured pixels to greyscale using the Leica QWin image analysis and processing software. This analysis was performed selecting random boxes including the extra- and intra-cellular space across the membrane, and the linear intensity of the signal was spatially recorded. We sampled three areas per each cell, and we repeated this on 30 different cells per experimental condition. The graphs in Fig. 1A show sample boxes used for the measure. These measures allowed to identify the thickness of the membrane, that is shown throughout the time-course in Fig. 1B, as well as the mean ± SD intensity of the actin staining in the membrane, in the cytosol, as well as the membrane/cytosol ratio (Fig. 1C).

Estrogen receptor recruitment turns into a rapid activation of the actin-regulatory protein moesin

Activation of ER with E2 turned into a rapid increase of Thr^{558} phosphorylation (which corresponds to activation) [15,16] of the actin-binding protein moesin (Fig. 2A). The activation of moesin by E2 follows the same kinetics as actin rearrangement (Fig. 2A) and was achieved through extra-nuclear pathways, as no changes of cell immunoreactive moesin were found (Fig. 2A). In estrogen-receptor negative MDA-MB-468 breast cancer cells moesin was constitutively phosphorylated and exposure to estradiol did not alter this activation any further, suggesting that this protein may be basally over-active in these cells (Fig. 2B).

In T47-D breast cancer cells, the activation of moesin was related to the concentration of E2 and was triggered by physiological amounts of the steroid (Fig. 2C), whereas in MDA-MB-468 cells no change in moesin phosphorylation was detected throughout all the range of estradiol concentrations (Fig. 2D).

Moesin is required for estrogen receptor-induced actin remodeling

To assess whether moesin is required for the estrogen receptor-dependent cytoskeletal rearrangement in T47-D cells, we silenced moesin by transfection of specific antisense phosphorotioate oligonucleotides (PONs) and observed the actions of E2 on actin rearrangement. Moesin expression was significantly reduced when T47-D breast cancer cells were transfected with antisense moesin PONs for 72 h (Fig. 3A). In moesin-silenced cells, E2 failed to induce a rapid actin reorganization, to induce increased in membrane thickness and to increase the ratio of membrane/cytosol actin staining (Fig. 3B-C). Furthermore, moesin-silenced cells did not develop specialized membrane structures in the presence of E2 (Fig. 3B). As control, E2 was fully effective in cells transfected with sense (inactive) moesin PONs (Fig. 3B-C).

Estrogen activates moesin via ERα

Moesin activation induced by E2 in T47-D cells was prevented by the addition of the pure ER antagonist ICI 182,780 (ICI, 1 μM) (Fig. 4A), indicating that ER is required. ICI 182,780 had no inhibitory effect on moesin phosphorylation in ER- MDA-MB-468 cells, supporting the concept that in these cells the recruitment of this protein does not require the presence of ER (Fig. 4B).

To identify which ER isoform is required for the signaling of estrogen to moesin, we treated T47-D cells with estradiol or with the preferential ERα agonist 4,4',4"-(4-propyl-[1H]-pyrazole-1,3,5-triyl)*tris*phenol (PPT, 1nM) [17] or with the ERβ agonist 2,3-*bis*(4-hydroxyphenil)-propionitrile (DPN, 1nM)[18]. Moesin activation was detected only in the presence of estradiol or PPT, suggesting that ERα supports the signaling to moesin, while ERβ is not required (Fig. 4C).

Since the ER isoform selectivity of PPT and DPN is not absolute (at higher concentrations they bind to some extent both ERα and ERβ), we knocked out ERα in T47-D cells with targeted small interfering RNAs (siRNAs). Transfection of the ERα siRNAs resulted in a clear reduction of ERα expression, along with a dramatic decrease of the phosphorylation of moesin during exposure to estrogen (Fig. 4D). This happened in the absence of modifications of the expression of moesin or ERβ (Fig. 4D), supporting the hypothesis that ERα drives the signaling of estradiol to moesin.

ERα signals to moesin through a $G\alpha_{13}$- and RhoA-dependent signaling pathway

In the search for the signaling pathways through which ERα leads to moesin activation in breast cancer cells, we used different pharmacological inhibitors linked to ERα or moesin. PD98059 (PD, 5 μM), an inhibitor of mitogen-activated protein kinases (MAPK) and wortmannin (WM, 30 nM), an inhibitor of phosphatidylinositol 3-OH kinase (PI3K), did not alter the estradiol-induced moesin phosphorylation (Fig. 5A). Instead, the G protein inhibitor, pertussis toxin (PTX, 100 ng/mL) significantly inhibited moesin phosphorylation induced by E2 (Fig. 5A). Moreover, the membrane-impermeable estradiol-bovine serum albumin conjugate (E2-BSA, 10 nM) triggered moesin activation similar to normal E2 (Fig. 5A). These findings suggest that a G protein-dependent, cell-membrane initiated mechanism mediates the signaling of ERα to moesin and to the actin cytoskeleton.

We previously showed that ERα is able to interact with the G protein, $G\alpha_{13}$, that controls the small GTPase RhoA and its effector, Rho-associated kinase (ROCK) [8]. This signaling cascade is implicated in the control of the cytoskeleton in human vascular cells [8]. With co-immunoprecipitation assays we found that in T47-D cells estradiol triggers a direct association of ERα with $G\alpha_{13}$ which is prevented by ICI 182,780 (Fig. 5B). In parallel, no co-immunoprecipitation of ERβ with $G\alpha_{13}$ was found (Fig. 5B).

By assaying RhoA GTP-binding activity, we found that RhoA is activated in T47-D cells by rapid exposure to estradiol or to the membrane-impermeable estradiol-BSA (Fig. 5C). RhoA activation was prevented by ER antagonism with ICI 182,780 and by interference with G proteins with PTX (Fig. 5C). The ERα-selective agonist PPT was associated with a strong activation of RhoA (Fig. 5C). The ERβ-preferential ligand, DPN, was also found to increase RhoA GTP-binding, although to a lesser extent (Fig. 5C).

To further test the requirement of $G\alpha_{13}$ and RhoA for ERα-induced moesin activation in T47-D breast cancer cells, we performed transient transfections with $G\alpha_{13}$ ($G\alpha_{13}$ Q226L) or RhoA (RhoA G14V) constitutively active mutated constructs or with $G\alpha_{13}$ (Gα13 Q226L/D294N) or RhoA (RhoA T19N) dominant negative constructs (Fig. 5D). Breast cancer cells transfected with constitutively active constructs showed an over-active moesin phosphorylation that was independent of estradiol (Fig. 5D). Instead, dominant negative $G\alpha_{13}$ or RhoA constructs

significantly inhibited the estradiol-induced moesin activation (Fig. 5D). Overall, these results show that $G\alpha_{13}$ and RhoA are implicated in the signaling of ERα to moesin in breast cancer cells.

ERα and moesin phosphorylation: role of the Rho-associated kinase (ROCK-2)

ROCK-2 phosphorylates moesin on Thr^{558} in different cell types, leading to filamentous actin fibers polymerization [19]. Pre-incubation of T47-D breast cancer cells with the specific Rho-kinase inhibitor, Y-27632 (Y-27632, 10 μM) prevented the activation of moesin by estradiol, implying that ROCK-2 is required for estrogen signaling to moesin in breast cancer cells (Fig 6A).

In agreement, ER activation resulted in increased ROCK-2 kinase activity in T47-D breast cancer cells (Fig. 6B). This was suppressed by ICI 182,780, Y-27632 as well as by PTX (Fig. 6B), indicating that ER recruitment turns into a G protein-dependent ROCK-2 activation.

In addition, we previously showed that ERα is able to interact with and directly activate ROCK-2 in human endothelial cells [8]. In T47-D breast cancer cells, an enhanced interaction between ERα and ROCK-2 was found with co-immunoprecipitation experiments in cells exposed to E2 (Fig. 6C-D). This protein-protein interaction was blocked by ICI 182,780 but not by PTX (Fig. 6C-D), suggesting that this may represent an additional mechanism for ERα-dependent ROCK-2 recruitment. To check whether the interaction with ERα turns ROCK-2 into an active status, we performed kinase assays using ERα immunoprecipitates (IPs) to target for Thr-phosphorylation the bait protein, myelin basic protein (MBP). ERα immunoprecipitates obtained from T47-D cells treated with estradiol induced MBP phosphorylation (Fig. 6E). ICI 182,780 and the ROCK-2 inhibitor Y-27632 counteracted this activation (Fig. 6E), confirming that ROCK-2 interacting with the ligand-engaged ERα is functionally activated. Consistently with the previous results, PTX did not reduce the activity of the ERα-associated-ROCK-2 (Fig. 6E), further suggesting the presence of two separate pathways of activation of ROCK-2 by ERα: one is G protein-dependent, while the second relies on a direct ERα/ROCK-2 interaction, which is not sensitive to PTX.

$G\alpha_{13}$, RhoA and ROCK-2 are necessary for the ER-dependent actin remodeling

To investigate whether $G\alpha_{13}$, RhoA or ROCK-2 are required for the ER-induced cytoskeletal remodeling, we studied the architecture of actin fibers while transfecting T47-D cells with the $G\alpha_{13}$ or RhoA mutated constructs or in the presence of the ROCK-2 inhibitor Y-27632. Both the $G\alpha_{13}$ and RhoA constitutively active constructs triggered a visible actin cytoskeleton remodeling with generation of membrane protrusions, resulting in enhanced interaction of T47-D cells with the

extracellular matrix and with nearby cells (Fig. 7A). Estradiol did not modify the cytoskeletal structure any further in these cells (Fig. 7A). In parallel, the dominant negative $G\alpha_{13}$ and RhoA constructs completely abrogated the modifications of actin and cell morphology induced by estrogen (Fig. 7A). Moreover, the inhibition of ROCK with Y-27632 completely prevented the effect of estradiol on cytoskeleton remodeling (Fig. 7A). These changes were reflected in the measurements of the mean membrane intensity and membrane/cytosol ratio (Fig. 7B).

The changes in actin spatial organization were accompanied by parallel modifications of the ratio between globular and fibrillar actin. At baseline, actin fibers predominantly existed as monomers (G-actin) (Fig. 7C). After treatment with E2 for 15 min, a visible shift from G to F actin was seen (Fig. 7C), indicating that ER recruitment is linked to polymerization of G-actin into F-actin. The ER antagonist ICI 182,780, the G protein inhibitor, pertussis toxin (PTX) and the Rho-kinase inhibitor Y-12732 largely prevented the shift from G- to F-actin induced by estradiol (Fig. 7C).

Recruitment of ER enhances breast cancer cell migration and invasion through a G protein/ROCK/moesin pathway

To address the question of the relevance of the ERα/$G\alpha_{13}$/RhoA/ROCK/moesin signaling cascade on breast cancer cell movement, we pretreated T47-D or MDA-MB-468 (ER-) breast cancer cells with cytosine arabinoside (1-(β-D-arabino-furanosyl)-cytosine hydrochloride - Ara-C, 100μM), an inhibitor of DNA strand separation that prevents cell division, and we performed horizontal migration assays. Estradiol (E2, 10 nM) strongly enhanced the migration of T47-D cells (Fig. 8). This was largely prevented by ICI 182,780, PTX and Y-27632, as well as by moesin silencing with antisense oligonucleotides (Fig. 8). In addition, the selective estrogen receptor modulator tamoxifen (TAM, 10 nM) that is used in the adjuvant treatment of ER+ breast cancers, also reduced the migration of T47-D cells induced by E2 while being ineffective on its own (Fig. 8).

In general, ER- MDA-MB-468 cells showed a stronger tendency to migrate in comparison to T47-D cells and this was not affected by E2, ICI, PTX or tamoxifen (Fig. 9). However, the ROCK inhibitor, Y-27632, significantly decreased the migration of these cells (Fig. 9), suggesting that ROCK-2 may be overactive in MDA-MB-468 cells, and that this may enhance their ability to migrate.

To test the impact of the ER-dependent signaling to moesin on breast cancer cell invasion we performed three-dimensional invasion assays using matrigel. Ara-C-pretreated cells showed an

enhanced invasion of the matrix in the presence of E2 or E2-BSA (Fig. 10). The effect of E2 was blocked by the ER-antagonist ICI 182,780, by PTX, by the ROCK-inhibitor Y-27632 as well as by tamoxifen (Fig. 10). In addition, transfection of moesin antisense PONs also resulted in impaired migration in the presence of estradiol (Fig. 10).

Moesin and P-moesin sub-cellular localization in normal breast tissue, benign breast disease and invasive breast cancer

To further characterize the biological role of moesin, we studied the sub-cellular distribution of wild-type moesin and activated moesin in normal and tumoral human breast tissues by immunochemistry.

In normal human mammary ducts, stainings for wild-type and phosphorylated moesin were found on the apical surface of ductal epithelial cells (Fig. 11), consistent with the usual localization in polarized secretory cells [9]. In addition, both moesin and P-moesin stainings were present in occasional basal myo-epithelial elements and in endothelial cells (Fig. 11). Similar to normal breast tissue, in breast fibroadenomas (FAD) moesin and P-moesin were prominently localized at the cell membrane of epithelial elements (Fig. 11), along with occasional stromal and myo-epithelial cells.

In addition, in order to characterize moesin and P-moesin expression and distribution in invasive breast cancers, we stained samples from human ductal carcinomas (tumor stage: pT1c - size between 1 and 2 cm - see table 1) and we compared the pattern of staining of ER positive or negative cancers, with or without lymph node metastasis.

Different from normal breast tissues or fibroadenomas, invasive ductal carcinomas showed a deranged moesin and P-moesin cellular localization, with four main expression/distribution patterns. Some cancers showed a weak, focal expression of moesin (focal, less than 10% of the cells stain for moesin, Fig. 11). Other cancers instead showed an intense staining for moesin, but some had a strong expression of moesin at the cell membrane (Fig. 11), while others showed a mixed membrane/cytoplasmic staining (Fig. 11). Other tumors had instead a clear cytoplasmic moesin staining, in the absence of membrane localization (Fig. 11).

There was no significant statistical difference in the association of the type of staining with lymph node metastasis status in ER+ or ER- cancers. However, ER- tumors showed a statistically significant difference vs. ER+ cancers in wild-type moesin localization, having consistently no

membrane-only staining while displaying a constant cytoplasmic moesin (table 1). In addition, although this was not significant, ER- cancers with lymph node metastasis tended to display more frequently a cytoplasmic-only moesin staining, without any membrane localization positioning (table 1).

When P-moesin staining was studied, similar patterns of sub-cellular distribution were found in invasive cancers (focal vs. intense staining; membrane vs. membrane/cytoplasmic vs. cytoplasmic, Fig. 11), but there was no significant association with either ER or lymph node status (table 1).

DISCUSSION

Estrogens act as promoters of cell proliferation and movement in different tissue types, including the breast (2). This action is particularly relevant in the presence of estrogen receptor positive (ER+) breast cancers, that are driven to grow, invade and metastasize by endogenous or exogenous estrogens (4, 31). For these reasons, understanding the basis through which estrogens drive cancer cells to interact with the extracellular environment to enact movement and invasion heralds profound biological and medical implications.

We here show that estrogen enhances horizontal migration and invasion of three-dimensional matrices of ER+ breast cancer cells by recruiting the actin-binding protein, moesin. Moesin resides at the nexus of multiple pathways regulating cell attachment with the extracellular matrix and with nearby cells, cell motility and metastatic potential as well as cell survival. These functions are directed by moesin though the modulation of actin cytoskeleton/plasma membrane interactions.

Moesin activation by estrogen in breast cancer cells is linked to the rapid and dynamic remodeling of the actin cytoskeleton and to the formation of specialized cell membrane structures, such as pseudopodia and ruffles, that are involved in the interaction with the extracellular matrix and required for cell movement (9, 12). These actions are consistent with our previous observation of improved wound healing due to enhanced endothelial cell movement in the presence of estrogens, linked to the activation of moesin (13), as well as with the recently reported activation of cytoskeletal remodeling and cell migration by estrogens in endometrial cancer (32).

Our findings also strengthen the concept that the nongenomic signaling of estrogen receptor to ERM proteins and actin may be of general relevance for the determination of cell movement. Indeed, the actions described in this report occur within minutes without the need of activating gene expression (33) and are thereof dynamically shut off within 30 to 60 minutes. This makes sense in light of the established requirement of multiple, periodic, waves of actin remodeling and dynamic formation of anchorage sites to the extracellular matrix in order to accomplish cell movement (9, 12).

In addition, loss of stress fibers is associated with cancer cell transformation and metastasis (34). Thus, the cytoskeletal rearrangement induced by estradiol through moesin may in part explain the carcinogenic actions of this steroid in estrogen-sensitive breast cancers, along with the enhanced

metastatic behavior of such neoplasms in the presence of sex steroid hormones (35). In support of this, similar actions of estrogen linked to the regulation of the ERM protein ezrin have been described in estrogen-sensitive cancers (19, 36).

ER- breast cancers, such as MDA-MB-468 cells, are not sensitive to estrogen administration in terms of moesin activation and cell migration. However, these cells display a basal hyper-activation of moesin. In addition, a direct inhibitor of moesin phosphorylation (ROCK inhibitor) is highly effective in reducing MDA-MB-468 cell horizontal migration. These findings are intriguing, as they suggest that sustained moesin activation by ROCK might be an important player in the metastatic behavior of ER- breast cancer cells. This fits with a previous report of a prominent expression of moesin in ER- human breast tumors, related to the tendency to metastasize (37).

The mechanistic basis that supports estrogen signaling to moesin and the actin cytoskeleton is found in the recruitment of the $G\alpha_{13}$/RhoA/ROCK pathway by ERα. Similarly to what previously found in human endothelial cells (13), estrogen-bound ERα dynamically interacts with the G protein $G\alpha_{13}$ and triggers its activation. This leads to the recruitment of the small GTPase RhoA and of its downstream effector, ROCK-2, which is responsible for moesin phosphorylation. These signaling intermediates, including moesin, are all required for actin remodeling as well as breast cancer cell migration and invasion. Interestingly, ERβ does not support the interaction with $G\alpha_{13}$ nor it activates moesin. Overall, this further establishes the nongenomic ERα/$G\alpha_{13}$/RhoA/ROCK/moesin signaling cascade as an important controller of cell movement by estrogen in different cell types, including cancer cells.

We also find that human breast cancers display a deranged over-expression and over-activation of moesin respect to normal breast tissues and/or benign fibroadenomas. Although our observation is only descriptive and limited to a small sample of patients, it is remarkable to find some variations in the sub-cellular localization of moesin in different cancer types. For instance, we find a trend towards the loss of membrane localization of moesin in ER- vs. ER+ cancers, which calls for future work to further characterize if the overall expression of this protein or its sub-cellular positioning might be associated with different cancer biology or behavior. This would be consistent with what is already known for the parent ERM protein, ezrin. Ezrin has been consistently found to be over-expressed in invasive epithelial neoplasia, such as in estrogen-sensitive endometrial (38, 39) and breast carcinomas (18, 40), and in highly aggressive sarcomas as well (14, 17), being related in many of these studies to the presence of tumor metastasis.

In conclusion, the present results suggest that within the broader range of actions of estrogen receptors, nongenomic signaling to the actin cytoskeleton through the ERα/$G\alpha_{13}$/RhoA/ROCK/moesin cascade is relevant for the determination of estrogen-dependent breast cancer cell movement and invasion that are related to cancer metastasis. The characterization of these actions increase our understanding of the effects of estrogens on breast cancer progression and might be useful to develop new tools to interfere with the ability to diffuse locally or at distant sites of ER+ or ER- breast carcinomas.

REFERENCES

1. Jemal, A., Siegel, R., Ward, E., Murray, T., Xu, J., Smigal, C., and Thun, M. J. (2006) Cancer statistics, 2006. *CA Cancer J Clin* 56, 106-130
2. Ricketts, D., Turnbull, L., Ryall, G., Bakhshi, R., Rawson, N. S., Gazet, J. C., Nolan, C., and Coombes, R. C. (1991) Estrogen and progesterone receptors in the normal female breast. *Cancer Res* 51, 1817-1822
3. Kelsey, J. L., Gammon, M. D., and John, E. M. (1993) Reproductive factors and breast cancer. *Epidemiol Rev* 15, 36-47
4. Yager, J. D., and Davidson, N. E. (2006) Estrogen carcinogenesis in breast cancer. *N Engl J Med* 354, 270-282
5. Lauffenburger, D. A., and Horwitz, A. F. (1996) Cell migration: a physically integrated molecular process. *Cell* 84, 359-369
6. Hua, J. Y., and Smith, S. J. (2004) Neural activity and the dynamics of central nervous system development. *Nat Neurosci* 7, 327-332
7. Egger, G., Klemt, C., Spendel, S., Kaulfersch, W., and Kenzian, H. (1994) Migratory activity of blood polymorphonuclear leukocytes during juvenile rheumatoid arthritis, demonstrated with a new whole-blood membrane filter assay. *Inflammation* 18, 427-441
8. Kedrin, D., van Rheenen, J., Hernandez, L., Condeelis, J., and Segall, J. E. (2007) Cell motility and cytoskeletal regulation in invasion and metastasis. *J Mammary Gland Biol Neoplasia* 12, 143-152
9. Giannone, G., Dubin-Thaler, B. J., Dobereiner, H. G., Kieffer, N., Bresnick, A. R., and Sheetz, M. P. (2004) Periodic lamellipodial contractions correlate with rearward actin waves. *Cell* 116, 431-443
10. Ananthakrishnan, R., and Ehrlicher, A. (2007) The forces behind cell movement. *Int J Biol Sci* 3, 303-317
11. Theriot, J. A. (2000) The polymerization motor. *Traffic* 1, 19-28
12. Pollard, T. D., Blanchoin, L., and Mullins, R. D. (2000) Molecular mechanisms controlling actin filament dynamics in nonmuscle cells. *Annu Rev Biophys Biomol Struct* 29, 545-576
13. Simoncini, T., Mannella, P., and Genazzani, A. R. (2006) Rapid estrogen actions in the cardiovascular system. *Ann N Y Acad Sci* 1089, 424-430

14. Khanna, C., Wan, X., Bose, S., Cassaday, R., Olomu, O., Mendoza, A., Yeung, C., Gorlick, R., Hewitt, S. M., and Helman, L. J. (2004) The membrane-cytoskeleton linker ezrin is necessary for osteosarcoma metastasis. *Nat Med* 10, 182-186
15. Tsukita, S., and Yonemura, S. (1999) Cortical actin organization: lessons from ERM (ezrin/radixin/moesin) proteins. *J Biol Chem* 274, 34507-34510
16. Bretscher, A., Reczek, D., and Berryman, M. (1997) Ezrin: a protein requiring conformational activation to link microfilaments to the plasma membrane in the assembly of cell surface structures. *J Cell Sci* 110 (Pt 24), 3011-3018
17. Yu, Y., Khan, J., Khanna, C., Helman, L., Meltzer, P. S., and Merlino, G. (2004) Expression profiling identifies the cytoskeletal organizer ezrin and the developmental homeoprotein Six-1 as key metastatic regulators. *Nat Med* 10, 175-181
18. Elliott, B. E., Meens, J. A., SenGupta, S. K., Louvard, D., and Arpin, M. (2005) The membrane cytoskeletal crosslinker ezrin is required for metastasis of breast carcinoma cells. *Breast Cancer Res* 7, R365-373
19. Song, J., Fadiel, A., Edusa, V., Chen, Z., So, J., Sakamoto, H., Fishman, D. A., and Naftolin, F. (2005) Estradiol-induced ezrin overexpression in ovarian cancer: a new signaling domain for estrogen. *Cancer Lett* 220, 57-65
20. Ridley, A. J., Schwartz, M. A., Burridge, K., Firtel, R. A., Ginsberg, M. H., Borisy, G., Parsons, J. T., and Horwitz, A. R. (2003) Cell migration: integrating signals from front to back. *Science* 302, 1704-1709
21. Takenawa, T., and Suetsugu, S. (2007) The WASP-WAVE protein network: connecting the membrane to the cytoskeleton. *Nat Rev Mol Cell Biol* 8, 37-48
22. Lin, V. C., Ng, E. H., Aw, S. E., Tan, M. G., and Bay, B. H. (2000) Progesterone induces focal adhesion in breast cancer cells MDA-MB-231 transfected with progesterone receptor complementary DNA. *Mol Endocrinol* 14, 348-358
23. Song, R. X., McPherson, R. A., Adam, L., Bao, Y., Shupnik, M., Kumar, R., and Santen, R. J. (2002) Linkage of rapid estrogen action to MAPK activation by ERalpha-Shc association and Shc pathway activation. *Mol Endocrinol* 16, 116-127
24. Iontcheva, I., Amar, S., Zawawi, K. H., Kantarci, A., and Van Dyke, T. E. (2004) Role for moesin in lipopolysaccharide-stimulated signal transduction. *Infect Immun* 72, 2312-2320
25. Oshiro, N., Fukata, Y., and Kaibuchi, K. (1998) Phosphorylation of moesin by rho-associated kinase (Rho-kinase) plays a crucial role in the formation of microvilli-like structures. *J Biol Chem* 273, 34663-34666

26. Matsui, T., Maeda, M., Doi, Y., Yonemura, S., Amano, M., Kaibuchi, K., and Tsukita, S. (1998) Rho-kinase phosphorylates COOH-terminal threonines of ezrin/radixin/moesin (ERM) proteins and regulates their head-to-tail association. *J Cell Biol* 140, 647-657

27. Kraichely, D. M., Sun, J., Katzenellenbogen, J. A., and Katzenellenbogen, B. S. (2000) Conformational changes and coactivator recruitment by novel ligands for estrogen receptor-alpha and estrogen receptor-beta: correlations with biological character and distinct differences among SRC coactivator family members. *Endocrinology* 141, 3534-3545

28. Meyers, M. J., Sun, J., Carlson, K. E., Marriner, G. A., Katzenellenbogen, B. S., and Katzenellenbogen, J. A. (2001) Estrogen receptor-beta potency-selective ligands: structure-activity relationship studies of diarylpropionitriles and their acetylene and polar analogues. *J Med Chem* 44, 4230-4251

29. Jeon, S., Kim, S., Park, J. B., Suh, P. G., Kim, Y. S., Bae, C. D., and Park, J. (2002) RhoA and Rho kinase-dependent phosphorylation of moesin at Thr-558 in hippocampal neuronal cells by glutamate. *J Biol Chem* 277, 16576-16584

30. Jaffe, A. B., and Hall, A. (2005) Rho GTPases: biochemistry and biology. *Annu Rev Cell Dev Biol* 21, 247-269

31. Platet, N., Cathiard, A. M., Gleizes, M., and Garcia, M. (2004) Estrogens and their receptors in breast cancer progression: a dual role in cancer proliferation and invasion. *Crit Rev Oncol Hematol* 51, 55-67

32. Acconcia, F., Barnes, C. J., and Kumar, R. (2006) Estrogen and tamoxifen induce cytoskeletal remodeling and migration in endometrial cancer cells. *Endocrinology* 147, 1203-1212

33. Simoncini, T., and Genazzani, A. R. (2003) Non-genomic actions of sex steroid hormones. *Eur J Endocrinol* 148, 281-292

34. Pawlak, G., and Helfman, D. M. (2001) Cytoskeletal changes in cell transformation and tumorigenesis. *Curr Opin Genet Dev* 11, 41-47

35. Yager, J. D., and Davidson, N. E. (2006) Estrogen Carcinogenesis in Breast Cancer. *N Engl J Med* 354, 270-282

36. Achen, M. G., McColl, B. K., and Stacker, S. A. (2005) Focus on lymphangiogenesis in tumor metastasis. *Cancer Cell* 7, 121-127

37. Carmeci, C., Thompson, D. A., Kuang, W. W., Lightdale, N., Furthmayr, H., and Weigel, R. J. (1998) Moesin expression is associated with the estrogen receptor-negative breast cancer phenotype. *Surgery* 124, 211-217

38. Ohtani, K., Sakamoto, H., Rutherford, T., Chen, Z., Satoh, K., and Naftolin, F. (1999) Ezrin, a membrane-cytoskeletal linking protein, is involved in the process of invasion of endometrial cancer cells. *Cancer Lett* 147, 31-38

39. Ohtani, K., Sakamoto, H., Rutherford, T., Chen, Z., Kikuchi, A., Yamamoto, T., Satoh, K., and Naftolin, F. (2002) Ezrin, a membrane-cytoskeletal linking protein, is highly expressed in atypical endometrial hyperplasia and uterine endometrioid adenocarcinoma. *Cancer Lett* 179, 79-86

40. Sarrio, D., Rodriguez-Pinilla, S. M., Dotor, A., Calero, F., Hardisson, D., and Palacios, J. (2006) Abnormal ezrin localization is associated with clinicopathological features in invasive breast carcinomas. *Breast Cancer Res Treat*

TABLE LEGEND

Table 1. Immunohistochemical analysis of moesin and P-moesin in normal breast tissue, benign breast disease and breast cancers. Negative indicates visible staining in less than 1% of the cells. **Focal** indicates staining in less than 30% cells. **Intense** indicates diffused staining throughout the tissue. **Membrane (MEM)** indicates staining exclusively localized to the cell membrane in more than 90% of the cells; **membrane/cytoplasm (MEM/CYTO)** indicates staining both on the cell membrane as well as in the cytoplasm in more than 90% of the cells; **cytoplasm (CYTO)** indicates staining of the cytoplasm without any evident membrane staining in more than 90% of the cells. Staining patterns were independently adjudicated by two pathologists.

FIGURE LEGENDS

Fig. 1. Recruitment of ER induces a dynamic remodeling of the actin cytoskeleton and of the cell membrane in T47-D breast cancer cells. A) T47-D cells were treated for different times with E2 (10 nM). Actin fibers were stained with phalloidin linked to Texas Red (red labeling) and nuclei were counterstained with DAPI (blue labeling). Immunofluorescent analysis reveals the dynamic modifications of actin fibers through the time-course and the formation of specialized cell membrane structures. Green arrows indicate longitudinal fibers; light blue arrows indicate membrane ruffles; yellow arrows indicate pseudopodia. Rectangles indicate the analyzed area which was demonstrated by the corresponding upper graph. In the graph, the longitudinal axis represents the gray level and the horizontal axis indicates pixels. Yellow, red and blue areas indicate the extracellular, plasma membrane and cytoplasmic fraction, respectively. **B and C)** Analytic results obtained by using Leica QWin image analysis and processing software showing the mean thickness of the cell membrane as well as the intensity of actin staining in the cytoplasm, membrane or extracellular compartment after treatment with E2 (10 nM) for different times. The results are derived from the sampling of five areas of the cell membrane of thirty different random cells. The areas of minimum and maximum cell membrane thickness were always included. The results are the mean ± SD of the measurements. In **C)** * = $p < 0.05$ vs. Basal condition (0 min).

Fig. 2. ER recruitment results in the activation of the actin-binding protein, moesin. Protein extracts from T47-D (**A and C**) and MDA-MB-468 (**B and D**) breast cancer cells treated for different times with 10 nM E2 (**A and B**) or for 15 min with increasing concentrations of E2 (**C and D**) were assayed with western analysis for their overall content of wild type moesin (moesin) or Thr^{558}-phosphorylated moesin (P-moesin).

Fig. 3. Moesin is required for estrogen-induced cytoskeletal remodeling. A) T47-D cells were transiently transfected with antisense (2 μM antisense MOESIN) moesin phosphorotioate oligonucleotides (PONs) for 0, 60 or 72 hours and moesin expression was assayed with western analysis. **B and C)** T47-D cells were transiently transfected with vehicle or antisense (2 μM antisense MOESIN) or sense (2 μM sense MOESIN) moesin phosphorotioate oligonucleotides (PONs) for 72 hours and then treated for 15 min with 10 nM E2. Moesin expression was checked by staining with a specific Ab linked to FITC (green labeling). Actin fibers were stained with phalloidin-Texas Red (red labeling) and nuclei were counterstained with DAPI (blue labeling). **F)** shows the analytic results obtained by using Leica QWin image analysis and processing software showing the mean thickness of the cell membrane as well as the intensity of actin and moesin staining in the cytoplasm, membrane or extracellular compartment. The results are derived from the

sampling of five areas of the cell membrane of thirty different random cells. The areas of minimum and maximum cell membrane thickness were always included. The results are the mean ± SD of the measurements. * = $p < 0.05$ vs. vehicle-transfected control.

Fig. 4. Estrogen signals to moesin via ERα. T47-D (**A and C**) or MDA-MB-468 (**B**) cells were treated for 15 minutes with either E2 (10 nM), the preferential ERα agonist PPT (10 nM) or the preferential ERβ agonist, DPN (10 nM), in the presence or absence of the ER antagonist, ICI 182,780 (1 μM). Western analyses of wild-type moesin (moesin) or Thr^{558}-phosphorylated moesin (P-moesin) were performed. **D)** T47-D cells were transfected with siRNAs vs. ERα (siRNA ERα), with scrambled siRNAs or with vehicle, and protein analysis for ERα, ERβ, wild-type moesin (moesin) or Thr^{558}-phosphorylated moesin (P-moesin) was performed on cell lysates after treatment for 15 min with vehicle or 10 nM E2.

Fig. 5. ERα signals to moesin via $G\alpha_{13}$ and RhoA. A) T47-D cells were exposed for 15 min to 10 nM E2 or to E2 conjugated to bovine serum albumin (E2-BSA; 10 nM), in the presence or absence of the ER antagonist ICI 182,720 (ICI; 1 μM), of the MAPK inhibitor PD98059 (PD; 5 μM), of the PI3 kinase inhibitor wortmannin (WM; 30 nM) or of the G protein inhibitor, PTX (100 ng/ml). Wild-type moesin (moesin) or Thr^{558}-phosphorylated moesin (P-moesin) were assayed in cell extracts. **B)** T47-D cells were treated for 15 min with 10 nM E2 in the presence or absence of ICI 182,720 (ICI, 1 μM). Cell protein extracts were immunoprecipitated with an Ab. vs. $G\alpha_{13}$ and the IPs were assayed for co-immunoprecipitation of ERβ or ERα. The membrane was re-blotted for $G\alpha_{13}$ to show equal input. **C)** RhoA activity was assayed in T47-D treated for 15 min with 10 nM E2, E2 conjugated to BSA (E2-BSA, 10 nM), the ERα-preferential ligand PPT (10 nM) or the ERβ-preferential agonist DPN (10 nM) in the presence or absence of ICI 182,720 (ICI, 1 μM) or PTX (100 ng/ml). Active, GTP-bound, RhoA was precipitated with Rhotekin, and a western analysis for RhoA was then performed. **D)** Whole-cell extracts were assayed for wild-type (moesin) or for Thr^{558}-phosphorylated (P-moesin) moesin content after transfection with empty vector or with $G\alpha_{13}$ or RhoA constitutively active ($G\alpha_{13}$ CA and RhoA CA) or dominant-negative ($G\alpha_{13}$ DN and RhoA DN) constructs, in the presence or absence of E2 (10 nM; 15 min).

Fig. 6. ERα recruits the Rho-associated kinase, ROCK-2. T47-D cells were treated for 15 min with 10 nM E2 in the presence or absence of the ROCK-2 inhibitor, Y-27632 (Y; 10 μM), ICI 182,720 (ICI; 1 μM), or PTX (100 ng/ml). **A)** Wild-type moesin (moesin) or Thr^{558}-phosphorylated (P-moesin) moesin were assayed in breast cancer cell extracts. **B)** Breast cancer cell protein extracts were immunoprecipitated with an Ab. vs. ROCK-2 and the IPs were used to perform kinase assays using de-phosphorylated myelin basic protein (MBP) as a bait. The lower box shows phosphorylation of MBP, the upper box shows the re-blot of the membranes for the immunoprecipitated protein. **C and D)** Breast cancer cell protein extracts were immunoprecipitated with an Ab. vs. ERα **(C)** or ROCK-2 **(D)** and co-immunoprecipitation of ROCK-2 or ERα was assayed with western analysis. The membranes were re-blotted for ERα or ROCK-2 to show equal

input. **E)** Breast cancer cell protein extracts were immunoprecipitated with an Ab. vs. ERα and the IPs were used to perform kinase assays using de-phosphorylated myelin basic protein (MBP) as a bait. The lower boxes show phosphorylation of MBP, the upper boxes show the re-blot of the membranes for the immunoprecipitated protein.

Fig. 7. Actin remodeling by estrogen receptor requires $G\alpha_{13}$, RhoA and ROCK-2. A) T47-D cells transiently transfected with either empty vector or with plasmids encoding for constitutively active or dominant-negative $G\alpha_{13}$ ($G\alpha_{13}$ CA or $G\alpha_{13}$ DN) or RhoA (RhoA CA or RhoA DN) were treated for 15 min with 10 nM E2. Other cells also received a co-treatment with E2 (10 nM; 15 min) and the ROCK inhibitor Y-27632 (Y; 10 μM). Breast cancer cell actin fibers were stained with phalloidin linked to Texas Red, and nuclei were counterstained with DAPI. **B)** shows the analytic results obtained by using Leica QWin image analysis and processing software showing the mean thickness of the cell membrane as well as the intensity of actin staining in the cytoplasm, membrane or extracellular compartment. The results are derived from the sampling of five areas of the cell membrane of thirty different random cells. The areas of minimum and maximum cell membrane thickness were always included. The results are the mean ± SD of the measurements. * = $p < 0.05$ vs. vehicle-transfected control. **C)** shows the changes of the amount of filamentous actin (F-actin, F) content versus free globular-actin (G-actin, G) content in T47-D cells after treatment with E2 (10 nM) for 15 min, in the presence or absence of ER antagonist ICI 182,720 (ICI; 1 μM), G protein inhibitor PTX (100 ng/ml) and ROCK-2 inhibitor Y-27632 (Y; 10 μM). Positive (Pos) and negative (Neg) controls were set by adding F-actin enhancing solution (phalloidin, 1 μM) or F-actin depolymerization solution (10 μM cytochalasin-D) to the lysates, respectively.

Fig. 8. Role of the G protein/ROCK/moesin pathway for ER+ breast cancer cell migration. Steroid-deprived, growth synchronized ER+ T47-D cells were exposed to 10 nM E2, in the presence or absence of the ER antagonist ICI 182,720 (ICI; 1 μM), of the G protein inhibitor PTX (100 ng/ml), or of the ROCK-2 inhibitor, Y-27632 (Y; 10 μM) or of the selective estrogen receptor modulator (SERM) tamoxifen (TAM, 10 nM). In addition, some T47-D cells were treated with 10 nM E2 in the presence or absence of transfection with sense (Sense; 2 μM) or antisense (AS; 2 μM) moesin phosphorotioate oligonucleotides (PONs). Breast cancer cells were scraped from the culture dish and the mean migration distance of the cells from the starting line was assayed after 48 h and expressed as mean ± SD. Representative images are shown and the mean ± SD of migration are shown in the bar graphs. * = $p < 0.05$ vs. E2.

Fig. 9. Role of the G protein/ROCK/moesin pathway for ER- breast cancer cell migration. ER- MDA-MB-468 cells were exposed to 10 nM E2, in the presence or absence of the ER antagonist ICI 182,720 (ICI; 1 μM), of the G protein inhibitor PTX (100 ng/ml), or of the ROCK-2

inhibitor, Y-27632 (Y; 10 μM) or of the selective estrogen receptor modulator (SERM) tamoxifen (TAM, 10 nM). Breast cancer cells were scraped from the culture dish and the mean migration distance of the cells from the starting line was assayed after 48 h and expressed as mean ± SD. Representative images are shown and the mean ± SD of migration are shown in the bar graphs. * = $p < 0.05$ vs. control.

Fig. 10. Role of the G protein/ROCK/moesin pathway for ER+ breast cancer cell invasion. Steroid-deprived, growth synchronized ER+ T47-D cells were exposed to 10 nM E2, or 10 nM E2-BSA conjugate in the presence or absence of the ER antagonist ICI 182,720 (ICI; 1 μM), of the G protein inhibitor PTX (100 ng/ml), or of the ROCK-2 inhibitor, Y-27632 (Y; 10 μM) or of the selective estrogen receptor modulator (SERM) tamoxifen (TAM, 10 nM). In addition, some T47-D cells were treated with 10 nM E2 in the presence or absence of transfection with sense (Sense; 2 μM) or antisense (AS; 2 μM) moesin phosphorotioate oligonucleotides (PONs). Breast cancer cell invasion through matrigel was assayed by using invasion chambers. Invading cells were counted in the central field of triplicate membranes. Invasion indexes and representative images in chambers with matrigel are shown. * = $p < 0.05$ vs. E2.

Fig. 11. Moesin and P-moesin expression and sub-cellular localization in human normal breast tissue, benign fibroadenomas and breast cancers. Histological sections (4 μm) from normal mammary glands, fibroadenomas or ER positive (ER+) breast cancers were used to identify the expression and localization of moesin and P-moesin with immunochemistry. Wild-type moesin as well as Thr^{558}-phosphorylated are shown as brown labeling. The figure displays sample images from the tumors analyzed in Table 1. Particularly, The normal breast tissue comes from Patient 2, the fibroadenomas is from patient 3. The breast cancer showing focal staining is that of patient 20, the cancer with membrane staining comes from patient 13. The cancer showing mixed membrane/cytoplasmic staining is from patient 17. The “high expression” cancer is from patient 12.

TABLE 1.

NORMAL BREAST											
SAMPLES				**MOESIN**	MEM	MEM/CITO	CYTO	**P-MOESIN**	MEM	MEM/CITO	CYTO
1				INTENSE	x			INTENSE	x		
2				INTENSE	x			INTENSE	x		
3				INTENSE	x			INTENSE	x		
4				INTENSE	x			INTENSE	x		
5				INTENSE	x			INTENSE	x		
FIBROADENOMAS											
SAMPLES				**MOESIN**	MEM	MEM/CITO	CYTO	**P-MOESIN**	MEM	MEM/CITO	CYTO
1				INTENSE	x			INTENSE	x		
2				INTENSE	x			INTENSE	x		
3				INTENSE	x			INTENSE	x		
4				INTENSE	x			INTENSE	x		
5				INTENSE	x			INTENSE	x		
INVASIVE DUCTAL CARCINOMAS											
SAMPLES	DIAMETER	pNx	ER%	**MOESIN**	MEM	MEM/CITO	CYTO	**P-MOESIN**	MEM	MEM/CITO	CYTO
ER POSITIVE/LYMPH NODE POSITIVE											
1	18 mm	pN2a (7/16)	84%	FOCAL	x			NEGATIVE			
2	19 mm	pN1m (1/8)	98%	INTENSE			x	INTENSE	x		
3	15 mm	pN1a (1/3)	98%	INTENSE	x			INTENSE	x		
4	16 mm	pN1a (2/24)	100%	INTENSE		x		FOCAL			x
5	16 mm	pN3a (8/15)	95%	INTENSE		x		FOCAL			x
ER POSITIVE/LYMPH NODE NEGATIVE											
1	14 mm		90%	INTENSE		x		FOCAL			x
2	15 mm		90%	INTENSE		x		INTENSE		x	
3	10 mm		100%	INTENSE	x			INTENSE		x	
4	15 mm		99%	FOCAL	x			INTENSE	x		
5	18 mm		98%	FOCAL	x			FOCAL	x		
ER NEGATIVE/LYMPH NODE POSITIVE											
1	18 mm	pN2a (7/16)	0%	FOCAL			x*	NEGATIVE			
2	17 mm	pN1m (1/17)	0%	INTENSE			x*	INTENSE		x	
3	11 mm	pN1m (1/1)	0%	INTENSE		x*		INTENSE	x		
4	17 mm	pN1a (2/19)	0%	INTENSE			x*	FOCAL			x
5	13 mm	pN3b (20/24)	0%	INTENSE		x*		FOCAL		x	
ER NEGATIVE/LYMPH NODE NEGATIVE											
1	8 mm		0%	INTENSE		x*		NEGATIVE			
2	16 mm		0%	INTENSE		x*		FOCAL			x
3	13 mm		0%	INTENSE		x*		FOCAL	x		
4	15 mm		0%	INTENSE			x*	NEGATIVE			
5	12 mm		0%	FOCAL		x*		INTENSE	x		

A

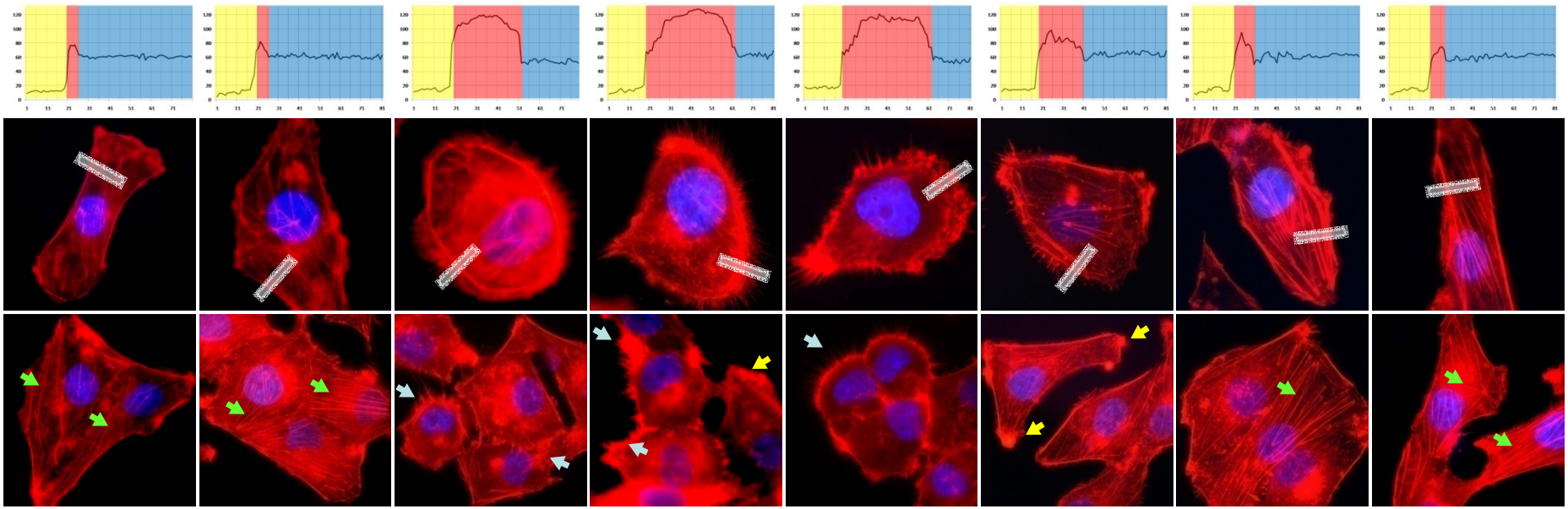

B

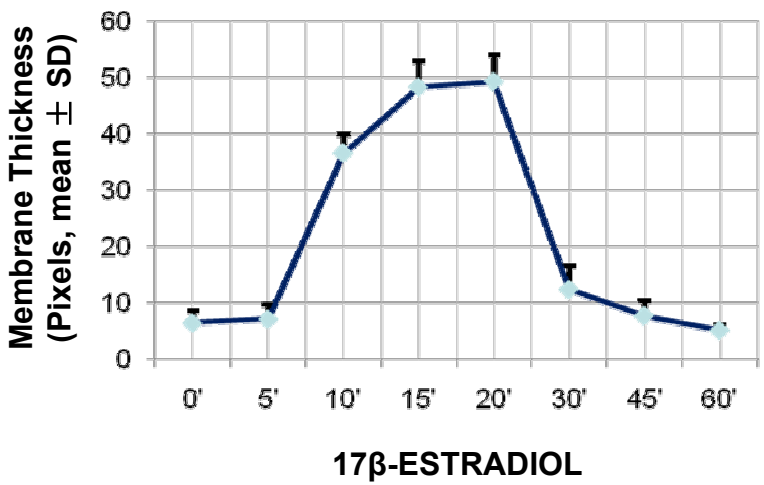

C

	MEAN MEMBRANE THICKNESS (pixel ± SD)	MEAN MEMBRANE INTENSITY (mean gray level ± SD)	MEAN CYTOSOL INTENSITY (mean gray level ± SD)	MEMBRANE/ CYTOSOL INTENSITY RATIO
0’	6,3 ± 2,1	62,3 ± 5,6	62,0 ± 7,8	1
5’	7,0 ± 2,6	75,4 ± 7,8	71,9 ± 7,8	1,1
10’	36,7 ± 14.5 *	120,5 ± 9,4 *	66,4 ± 2,8	1,8 *
15’	48,3 ± 4.7 *	114,7 ± 11,8 *	55,1 ± 9,0	2,1 *
20’	49,3 ± 4.7 *	112,4 ± 13,5 *	66,7 ± 2	1,7 *
30’	22,3 ± 4,2	96,4 ± 11,4 *	72,3 ± 4,9	1,3
45’	7,6 ± 2,8	71,1 ± 14,2	61,9 ± 2,5	1,1
60’	5,0 ± 1	61,5 ± 1,9	62,4 ± 2,2	0,99

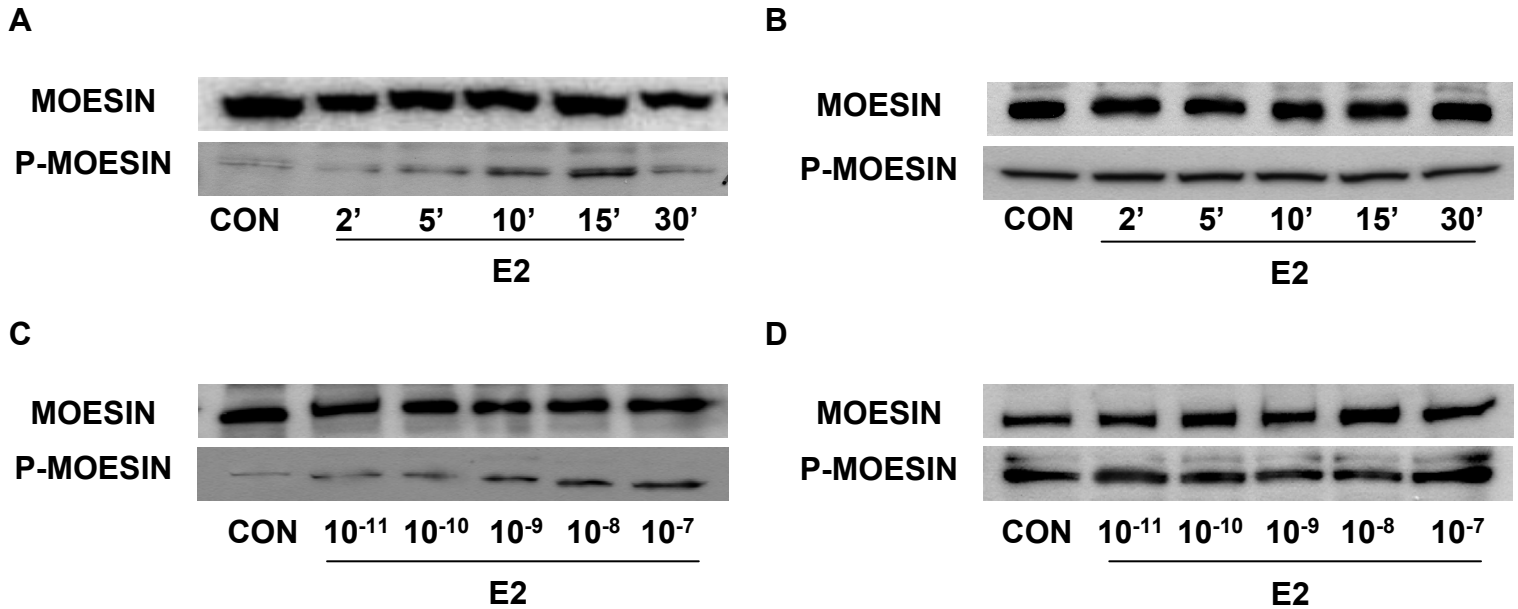
A
MOESIN
P-MOESIN
CON
2'
5'
10'
15'
30'
E2
B
MOESIN
P-MOESIN
CON
2'
5'
10'
15'
30'
E2
C
MOESIN
P-MOESIN
CON
10-11
10-10
10-9
10-8
10-7
E2
D
MOESIN
P-MOESIN
CON
10-11
10-10
10-9
10-8
10-7
E2

A

C

		MEAN CYTOSOL INTENSITY (MOESIN) (mean gray level ± SD)	MEAN MEMBRANE THICKNESS (ACTIN) (pixel ± SD)	MEAN MEMBRANE INTENSITY (ACTIN) (mean gray level ± SD)	MEAN CYTOSOL INTENSITY (ACTIN) (mean gray level ± SD)	MEMBR/ CYTOSOL INTENSITY RATIO (ACTIN)
	CON	97,6 ± 2,5	7,8 ± 1,7	61,2 ± 4,0	61,8 ± 5,8	0,99
	E2	103,0 ± 2,3	43,0 ± 5,6 *	118,5 ± 2,6 *	54,7 ± 3,9	2,2 *
AS	CON	19,5 ± 5,2 *	6,7 ± 0,5	57,3 ± 5,4	65,2 ± 7,7	0,9
	E2	21,1 ± 1,8 *	7,7 ± 0,7	73,5 ± 5,4	70,8 ± 2,7	1,04
S	CON	104,3 ± 1,7	8,3 ± 1,1	72,4 ± 13,5	66,8 ± 2,0	1,1
	E2	98,2 ± 3,6	42,3 ± 4,2 *	126,4 ± 11,4 *	52,3 ± 5,9	2,4 *

B

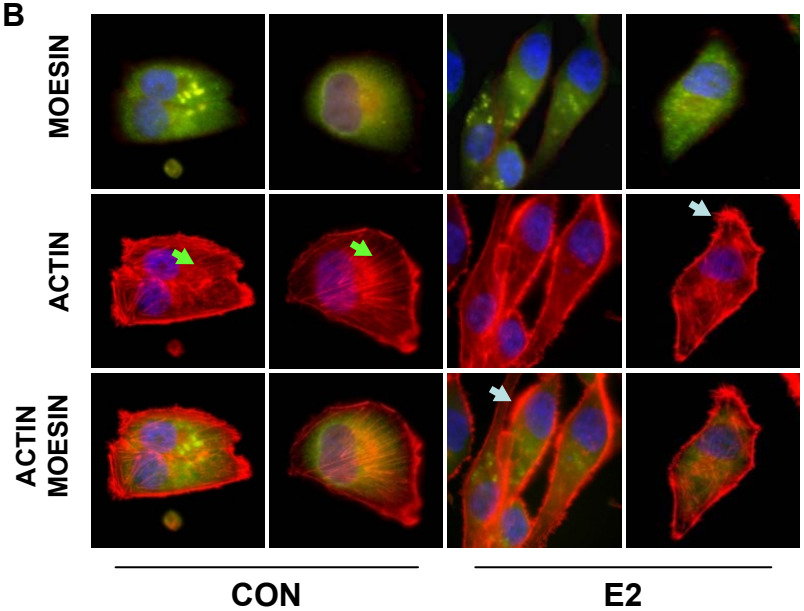

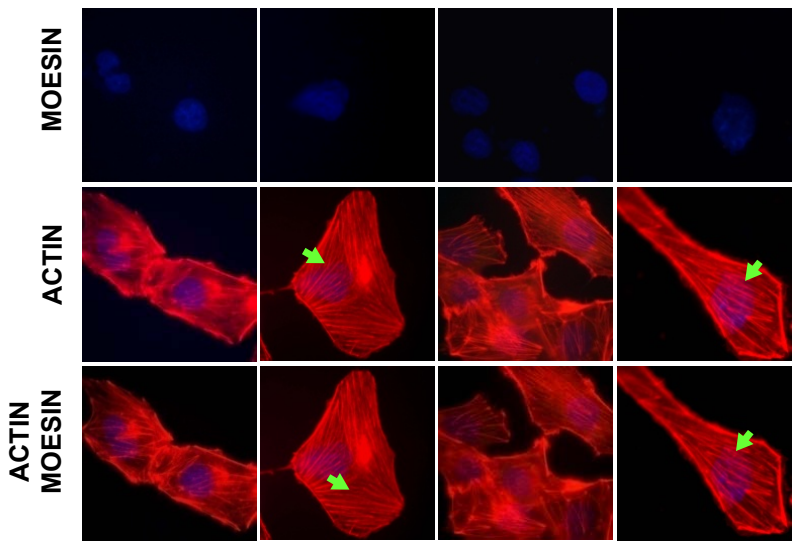

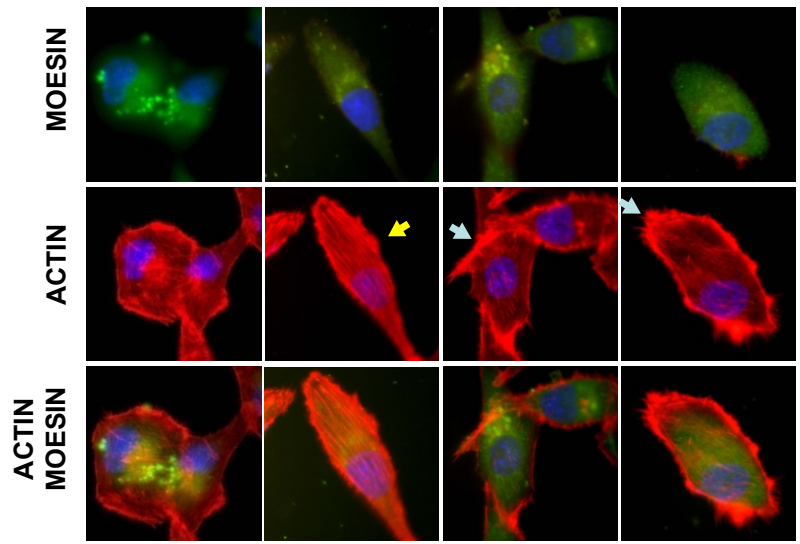

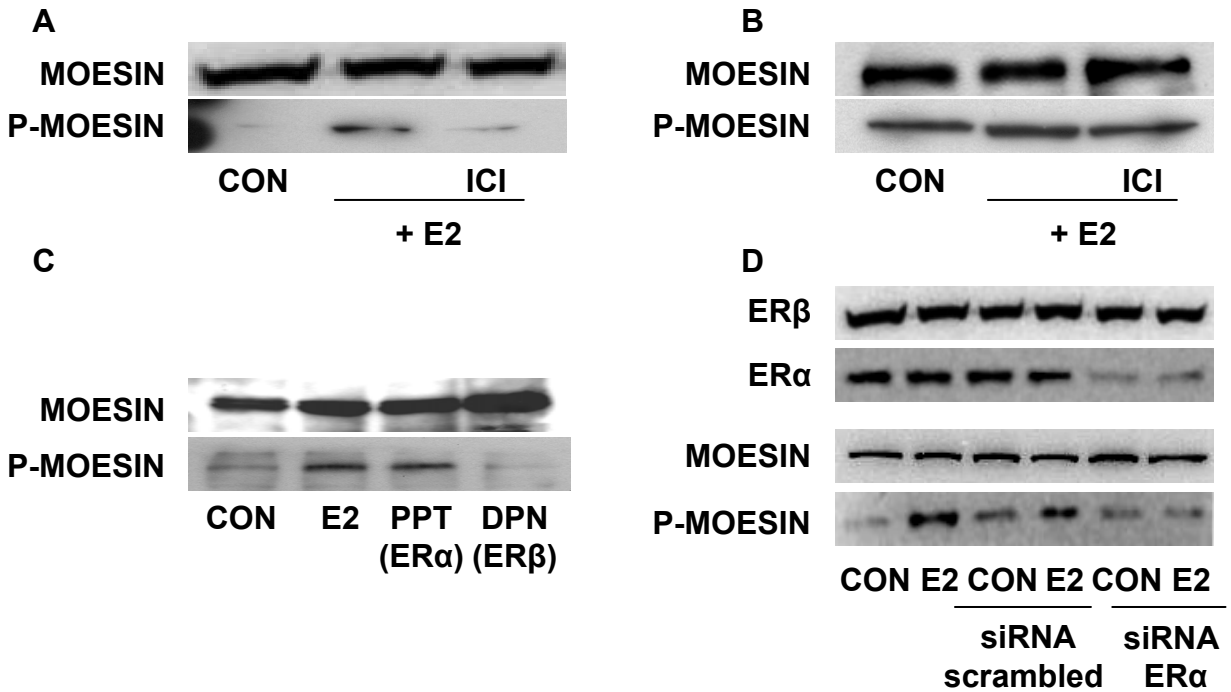
A
MOESIN
P-MOESIN
CON
ICI
+ E2
B
MOESIN
P-MOESIN
CON
ICI
+ E2
C
MOESIN
P-MOESIN
CON
E2
PPT (ERα)
DPN (ERβ)
D
ERβ
ERα
MOESIN
P-MOESIN
CON E2 CON E2 CON E2
siRNA scrambled
siRNA ERα

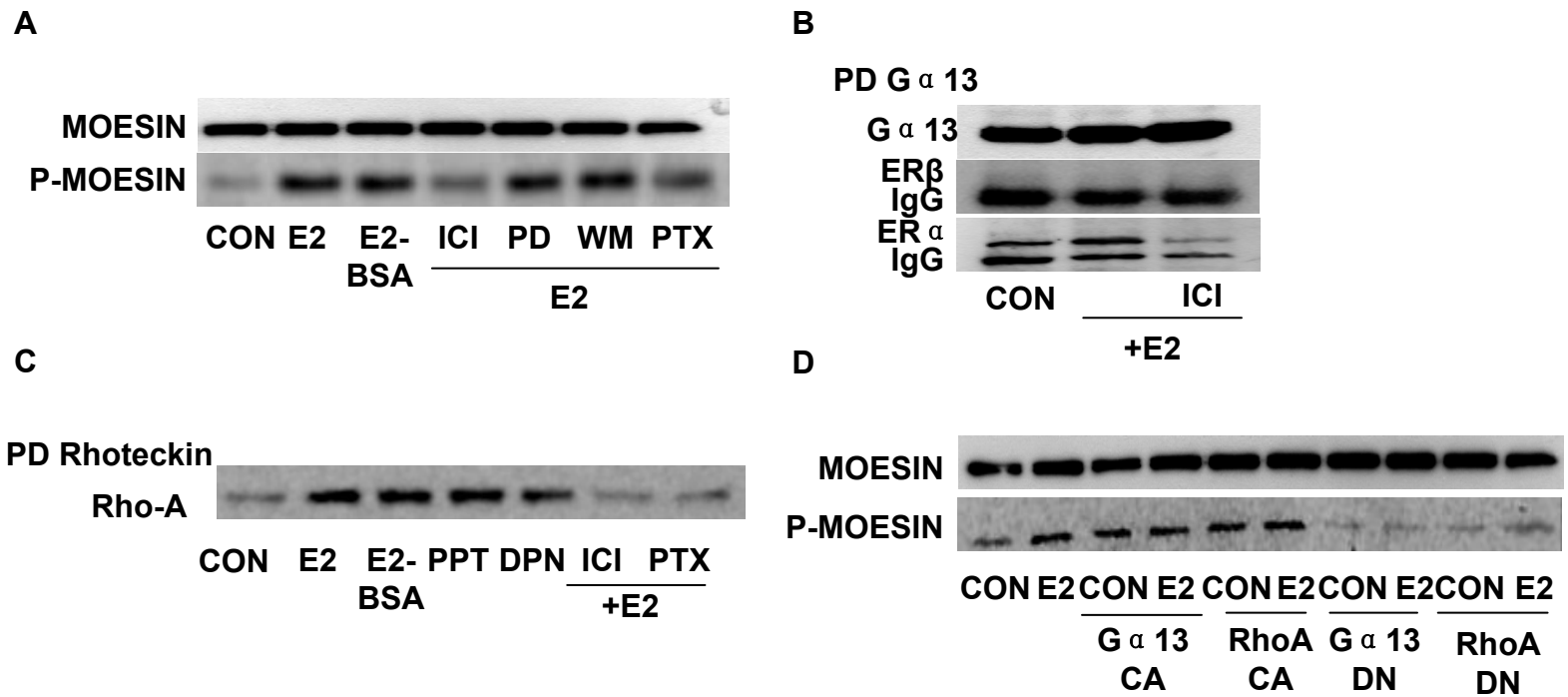
A
MOESIN
P-MOESIN
CON E2 E2-BSA ICI PD WM PTX
E2
B
PD G α 13
G α 13
ERβ IgG
ER α IgG
CON ICI
+E2
C
PD Rhoteckin
Rho-A
CON E2 E2-BSA PPT DPN ICI PTX
+E2
D
MOESIN
P-MOESIN
CON E2 CON E2 CON E2 CON E2 CON E2
G α 13 CA
RhoA CA
G α 13 DN
RhoA DN

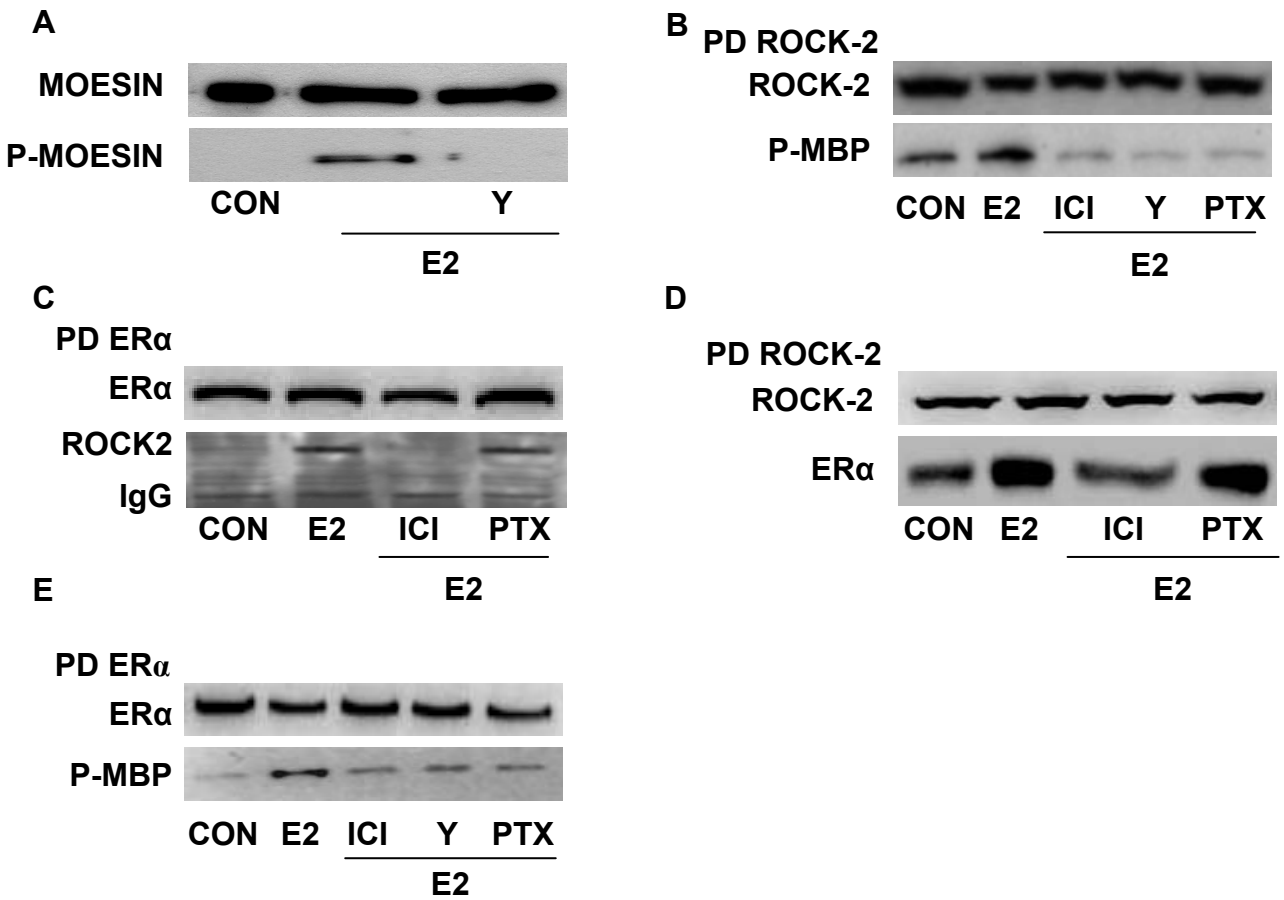
A
MOESIN
P-MOESIN
CON
Y
E2
B
PD ROCK-2
ROCK-2
P-MBP
CON E2 ICI Y PTX
E2
C
PD ERα
ERα
ROCK2
IgG
CON E2 ICI PTX
E2
D
PD ROCK-2
ROCK-2
ERα
CON E2 ICI PTX
E2
E
PD ERα
ERα
P-MBP
CON E2 ICI Y PTX
E2

M.S.Giretti et al. Fig. 7

A

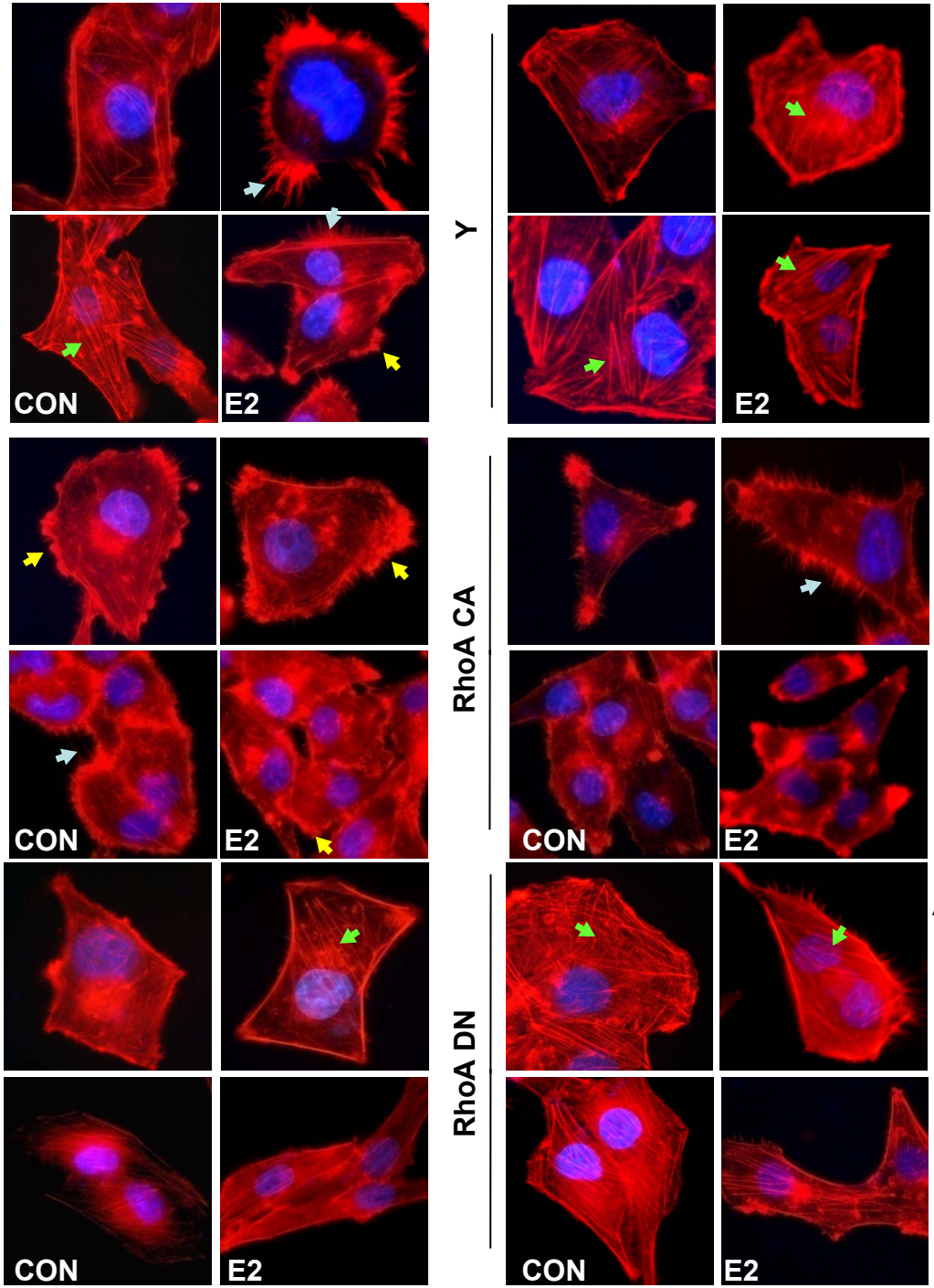

B

		MEAN MEMBRANE THICKNESS (ACTIN) (pixel ± SD)	MEAN MEMBRANE INTENSITY (ACTIN) (mean gray level ± SD)	MEAN CYTOSOL INTENSITY (ACTIN) (mean gray level ± SD)	MEMBR/ CYTOSOL INTENSITY RATIO (ACTIN)
	CON	7,8 ± 1,7	61,2 ± 4,0	61,8 ± 5,8	0,99
	E2	43,0 ± 5,6 *	118,5 ± 2,6 *	54,7 ± 3,9	2,2 *
Y	CON	6,7 ± 1,7	57,3 ± 5,4	65,2 ± 7,7	0,9
	E2	10,6 ± 2,5	70,5 ± 7,1	60 ± 7,4	1,2
Gα13 CA	CON	60,8 ± 5,1	121,9 ± 11,95 *	59± 9,9	2,1 *
	E2	61,4 ± 1,5	117,1 ± 7,9 *	55,9 ± 2,1	2,3 *
Gα13 DN	CON	7,8± 2,1	67,3± 3,2	68,1± 1,6	0,99
	E2	9,2± 1,04	72,4± 6,5	71,1± 4,9	1,02
RhoA CA	CON	56± 5,6	124,7± 2,8 *	67,9± 1,5	1,8 *
	E2	67± 6,2	118,2± 1,5 *	58,7± 2,9	2,1 *
RhoA DN	CON	6,5± 2,5	66,7 ± 9,1	71,8 ± 1,1	0,93
	E2	8,3 ± 0,9	76,2 ± 1,4	71,2 ± 1,4	1,07

C

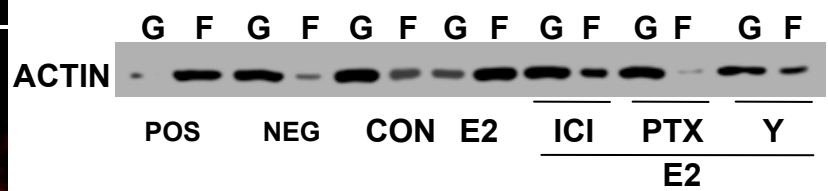

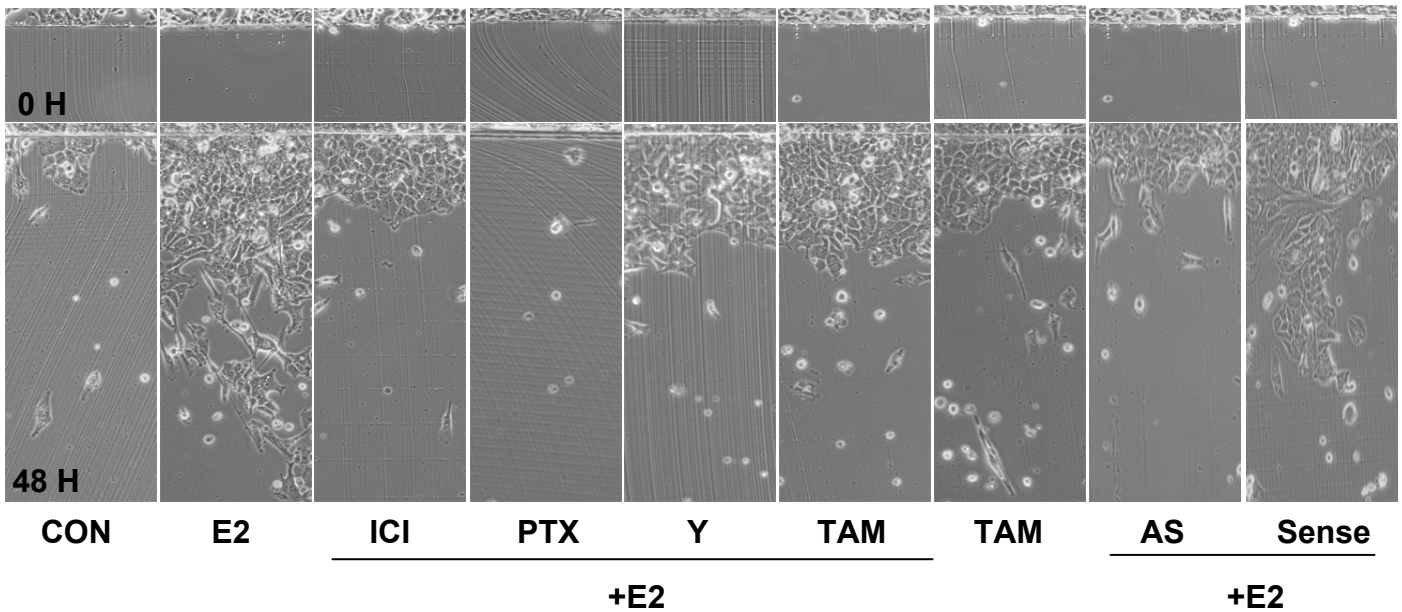
0 H
48 H
CON
E2
ICI
PTX
Y
TAM
TAM
AS
Sense
+E2
+E2

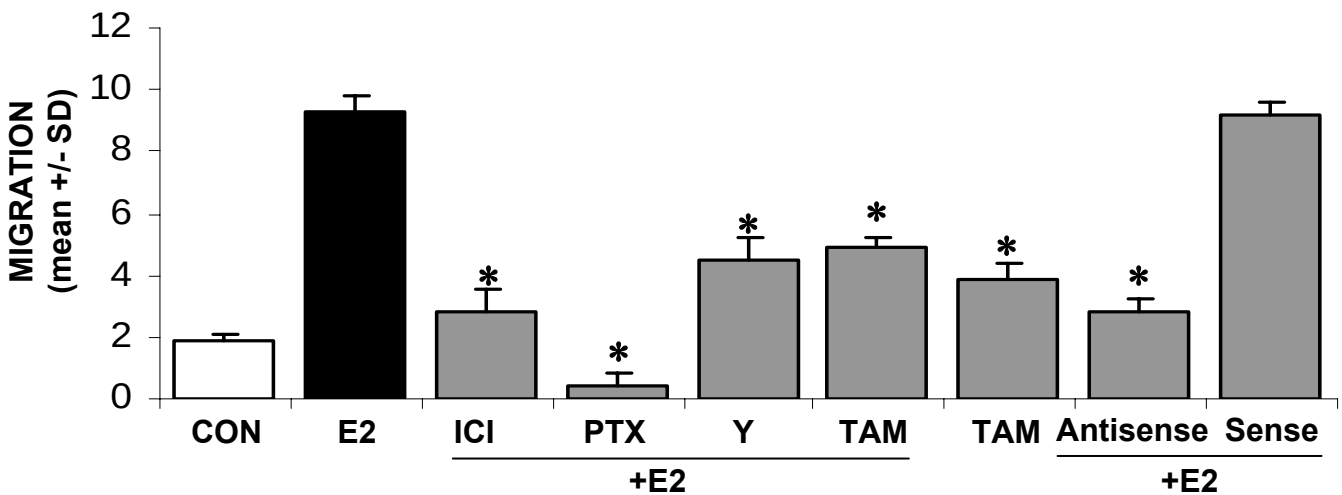
MIGRATION
(mean +/- SD)
12
10
8
6
4
2
0
CON
E2
ICI
PTX
Y
TAM
TAM
Antisense
Sense
+E2
+E2

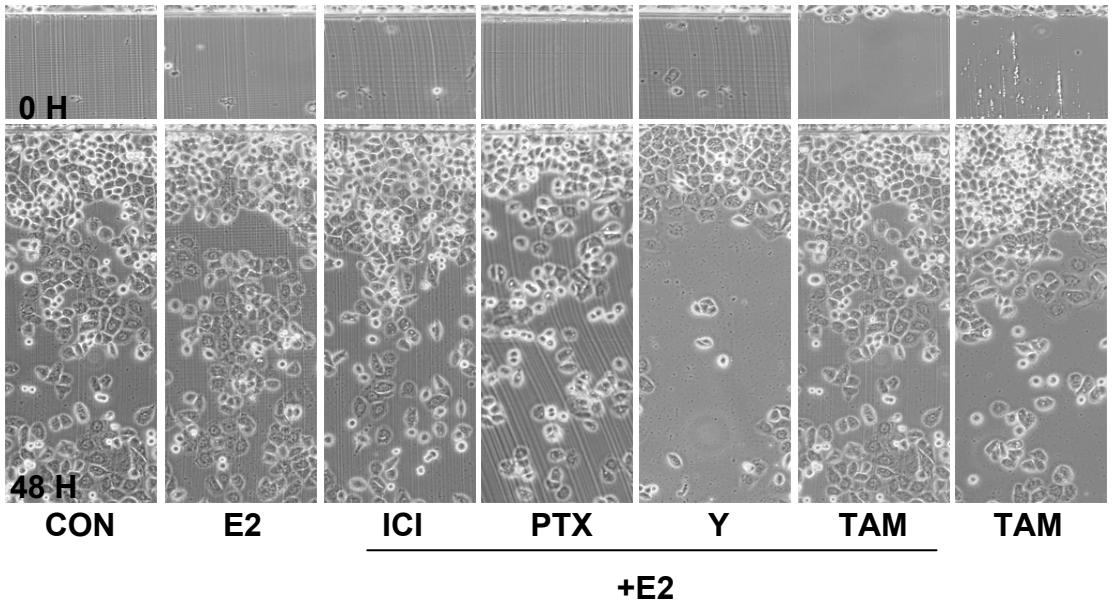
0 H
48 H
CON
E2
ICI
PTX
Y
TAM
TAM
+E2
MIGRATION
(mean +/- SD)
12
10
8
6
4
2
0
*
CON
E2
ICI
PTX
Y
TAM
TAM
+E2

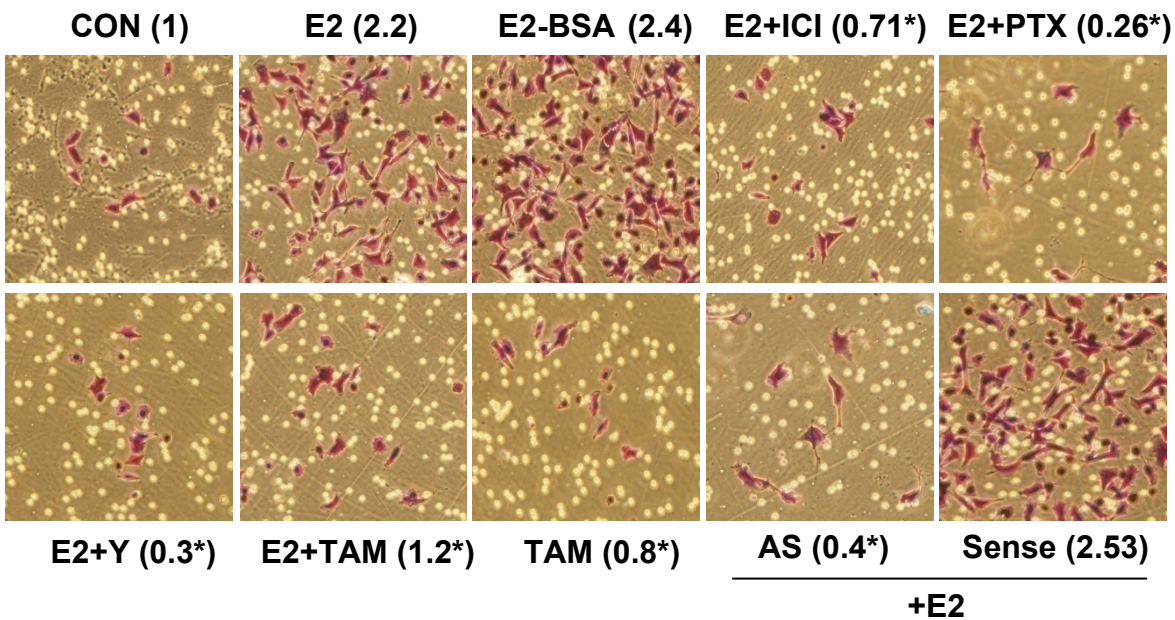
CON (1)
E2 (2.2)
E2-BSA (2.4)
E2+ICI (0.71*)
E2+PTX (0.26*)
E2+Y (0.3*)
E2+TAM (1.2*)
TAM (0.8*)
AS (0.4*)
Sense (2.53)
+E2

M.S.Giretti et al. Fig. 11